

# **SiC-Based Hydrogen Selective Membranes for Water-Gas-Shift Reaction**

**Final Technical Report**

**Reporting Period: 9/16/99 - 12/31/03**

**Paul K.T. Liu, Principal Investigator**

**December 2003**

**Award No. DE-FG26-99FT40683**

**Media and Process Technology Inc.  
1155 William Pitt Way  
Pittsburgh, PA 15238**

**Subcontractor:**

**University of Southern California  
University Park  
Los Angeles, CA 90089**

**Disclaimer**

This report was prepared as an account of work sponsored by an agency of the United States Government. Neither the United States Government nor any agency thereof, nor any of their employees, makes any warranty, express or implied, or assumes any legal liability or responsibility for the accuracy, completeness, or usefulness of any information, apparatus, product, or process disclosed, or represents that its use would not infringe privately owned rights. Reference herein to any specific commercial product, process, or services by trade name, trademark, manufacturer, or otherwise does not necessarily constitute or imply its endorsement, recommendation, or favoring by the United States government or any agency thereof. The view and opinions of authors expressed herein do not necessarily state or reflect those of the United States Government or any agency thereof.

## ABSTRACT

A hydrogen selective membrane as a membrane reactor (MR) can significantly improve the power generation efficiency with a reduced capital and operating cost for the water-gas-shift reaction. Existing hydrogen selective ceramic membranes are not suitable for the proposed MR due to their poor hydrothermal stability. In this project we have focused on the development of innovative silicon carbide (SiC) based hydrogen selective membranes, which can potentially overcome this technical barrier. SiC macro-porous membranes have been successfully fabricated via extrusion of commercially available SiC powder. Also, an SiC hydrogen selective thin film was prepared via our CVD/I technique. This composite membrane demonstrated excellent hydrogen selectivity at high temperature (~600°C). More importantly, this membrane also exhibited a much improved hydrothermal stability at 600°C with 50% steam (atmospheric pressure) for nearly 100 hours. In parallel, we have explored an alternative approach to develop a H<sub>2</sub> selective SiC membrane via pyrolysis of selected pre-ceramic polymers and sol-gel techniques. Building upon the positive progress made in the membrane development study, we conducted an optimization study to develop an H<sub>2</sub> selective SiC membrane with sufficient hydrothermal stability suitable for the WGS environment. In addition, mathematical simulation has been performed to compare the performance of the membrane reactor (MR) vs conventional packed bed reactor for WGS reaction. Our result demonstrates that >99.999% conversion can be accomplished via WGS-MR using the hydrogen selective membrane developed by us. Further, water/CO ratio can be reduced, and >97% hydrogen recovery and <200 ppm CO can be accomplished according to the mathematical simulation. Thus, we believe that the operating economics of WGS can be improved significantly based upon the proposed MR concept. In parallel, gas separations and hydrothermal and long-term-storage stability of the hydrogen selected membrane have been experimentally demonstrated using a pilot-scale tubular membrane under a simulated WGS environment.

## TABLE OF CONTENTS

	<u>Page</u>
1. EXECUTIVE SUMMARY .....	1
2. INTRODUCTION .....	3
2.1 Project Objectives .....	3
2.2 Macro- and Meso-Porous SiC Membranes as Substrates for SiC-H <sub>2</sub> Selective Membranes .....	4
2.3 Porous SiC Membranes via Prepyrolysis of Pre-Ceramic Polymers .....	4
2.4 H <sub>2</sub> Selective SiC Membranes via Chemical Vapor Deposition/Infiltration (CVD/I).....	5
2.5 Microporous SiC Membranes via Sol-Gel Approach .....	5
2.6 Product Development and Process Simulation for WGS .....	6
3. EXPERIMENTAL PROCEDURE .....	6
3.1 Macroporous SiC Membranes as Substrates for SiC-H <sub>2</sub> Selective Membranes.....	6
3.2 H <sub>2</sub> Selective SiC Membranes via Chemical Vapor Deposition/Infiltration (CVD/I).....	6
3.3 H <sub>2</sub> Selective SiC Membranes via Pyrolysis of Pre-ceramic Polymers .....	7
3.4 Microporous Membranes via Sol Gel Approach.....	7
3.5 Thermal and Hydrothermal Stability Test.....	8
4. RESULTS AND DISCUSSION .....	9
4.1 SiC Macro- and Meso-porous Membranes as Substrates .....	9
4.2 H <sub>2</sub> Selective SiC Membranes via Chemical Vapor Deposition/Infiltration (CVD/I).....	9
4.3 H <sub>2</sub> Selective SiC Membranes via Pyrolysis of Pre-ceramic Polymers .....	11
4.4 Microporous Membrane via Sol-Gel Approach.....	12
4.5 Product Development and Process Simulation for WGS .....	15
5. CONCLUSION .....	16
BIBLIOGRAPHY.....	61
LIST OF ACRONYMS AND ABBREVIATIONS .....	63
APPENDICES	
Publications as a result of current research under this project.....	64

## LIST OF TABLES AND FIGURES

### Tables

Table 1.	Helium and Nitrogen Permeances of Mesoporous SiC Membranes Prepared via Calcination of Polycarbosilane .....	19
Table 2.	Permeance of SiC membranes after CVD/I at 750°C and after calcination at 1,000°C.	20
Table 3.	Permeance vs. temperature for SiC H <sub>2</sub> -selective membranes prepared with CVD/I technique at 700°C.....	21

### Figures

Figure 1.	The cumulative particle and pore sizes distribution of substrate made from 1 $\Rightarrow$ (P1) average particle size powder. ....	22
Figure 2.	The permeability and separation factor of macroporous substrate (P1). ....	22
Figure 3.	SEM photomicrograph of top surface of SiC macroporous substrate (P1). ....	23
Figures 4.	Pore size distribution (based on BET measurement) of SiC film prepared from calcination of polycarbosilane. ....	23
Figure 5.	XRD pattern of SiC substrate prepared from calcination of polycarbosilane. ....	24
Figure 6.	SEM photomicrograph (of top surface) of SiC microporous substrate prepared from calcination of polycarbosilane. ....	24
Figure 7.	XRD pattern ( $\beta$ -SiC) of unsupported SiC thin film prepared with sol-gel technique. ....	25
Figure 8.	Pore size distribution (based upon N <sub>2</sub> adsorption)of SiC thin film prepared via sol-gel technique. ....	25
Figure 9.	Surface topograph of microporous SiC membrane prepared via sol-gel technique. ....	26
Figure 10.	Gas permeance (single component) and separation factor vs. transmembrane pressure drop of microporous SiC membrane supported on SiC macroporous substrate.. ....	27
Figure 11.	XRD pattern of SiC powder prepared from pre-ceramic polymer (AHPCS) calcined at 1,000 to 1,600°C. ....	28
Figure 12.	Calculated crystal size of the SiC powder prepared from pre-ceramic polymer (AHPCS) calcined at 1,000 to 1,600°C .....	29
Figure 13.	Effect of the number of coatings on the permeance and separation factor (at room	

temperature) of SiC H <sub>2</sub> selective membranes prepared from pre-ceramic polymer (AHPCS) coated on SiC macroporous substrate. ....	30
Figure 14. Pore size distribution (microporous range) of SiC powder prepared via pyrolysis (1 <sup>st</sup> , 2 <sup>nd</sup> and 3 <sup>rd</sup> ) of pre-ceramic powder .....	31-32
Figure 15. Pore size distribution (meso- and micro-porous range) of SiC powder prepared from pyrolysis of pre-ceramic polymer (AHPCS).....	33
Figure 16. Permeance of N <sub>2</sub> and He as a function of temperature obtained from SiC membrane prepared with pre-ceramic polymer (AHPCS) coated on SiC macroporous substrate. ...	34
Figure 17. Separation factor (He/N <sub>2</sub> ) as a function of temperature obtained from SiC H <sub>2</sub> selective membrane prepared with a pre-ceramic polymer (AHPCS) coated on SiC porous substrate. ....	35
Figure 18. XRD analysis of unsupported SiC films prepared via CVD/I at 750°C and calcined at 1,000 (bottom), 1,200 (middle), and 1,400°C (top).....	36
Figure 19a. SEM photomicrograph of M&P's alumina microporous substrate (ca. 100Å) with SiC thin film deposition via CVD/I. ....	37
Figure 19b. Higher magnification of Figure 19a. ....	37
Figure 20. SEM photomicrograph of the SiC membrane after oxidation at 400°C in air for two hours.....	38
Figure 21. Permeance and selectivity vs. temperature for one of the SiC membranes (TPS-006B).....	39
Figure 22. Permeance of SiC membrane at 450°C and 30% steam (membrane after poste-treated to remove excess carbon).....	40
Figure 23a. XRD pattern of SiC powder (prepared from Sol6) before the hydrothermal stability test at 350°C and 50% steam (ambient pressure base). ....	41
Figure 23b. .XRD pattern of SiC powder (prepared from Sol6) after the hydrothermal stability test at 350°C and 50% steam (ambient pressure).....	41
Figure 24. Pore size distribution of SiC powder (prepared from Sol6) before and after hydrothermal stability test at 350°C and 50% steam (ambient pressure).....	41
Figure 25a. Hydrothermal stability test of silicon carbon membrane (TPS-021) at 750°C and 50% steam (atmospheric pressure).....	42
Figure 25b. Helium and nitrogen permeance of SiO <sub>2</sub> membrane stability test at 600°C and 20%	

steam (for comparison) .....	42
Figure 26. Effect of thermal cycling on SiC membrane (TPS-006B) supported in Al <sub>2</sub> O <sub>3</sub> membrane: assessment of thermal mismatch between SiC and Al <sub>2</sub> O <sub>3</sub> .....	43
Figure 27 The TEM picture of the organo-silica sol type IPAST with particle size 8-11 nm, provided by Nissan Chemical Industries, Ltd. ....	44
Figure 28 The XRD pattern of a SiC powder treated with HF, air, and steam .....	45
Figure 29 The pore size distribution of the SiC powders after various treatment .....	46
Figure 30 The dV/dlogD of the SiC substrate utilized in the preparation of the sol-gel membrane .....	47
Figure 31 The argon permeance of the membrane as a function of the pressure gradient and the number of coatings .....	48
Figure 32 The separation factor of the membrane as a function of the pressure gradient and the number of coatings.....	49
Figure 33 The XRD patterns of the SiC membrane and the unsupported film (powder) prepared by the same techniques .....	50
Figure 34 Argon permeance of the SiC membrane in the presence of steam .....	51
Figure 35 A SEM picture of the cross section of the SiC membrane prepared by sol-gel technique .....	52
Figure 36 The XPS spectrum of the SiC powder sample .....	53
Figure 37 Performance of M&P Hydrogen Selective Membrane (U-130) and its Storage Stability (presented in terms of H <sub>2</sub> Permeance).....	54
Figure 38 Performance of M&P Hydrogen Selective Membrane and its Long Term Storage Stability (U-130): in terms of Nitrogen Permeance .....	55
Figure 39 Hydrothermal Stability Test of M&P Hydrogen Selective Membrane (200±5C with 3±-0.5bar steam) .....	56
Figure 40 Hydrogen purity plotted as a function of hydrogen recovery for a full-scale M&P hydrogen selective membrane at 150°C and 100 psig .....	57
Figure 41 CO Conversion in Packed bed vs Membrane Reactor .....	58

Figure 42	CO Conversion through WGS: Effect of Steam/CO Ratio.....	59
Figure 43	Effect of Steam/CO ratio for Hydrogen Recovery in Membrane reactor (same condition as above).....	60
Figure 44	CO Concentration in H <sub>2</sub> Recovered from Membrane Reactor (same condition as above)	60

## 1. EXECUTIVE SUMMARY

The concept of catalytic membrane reactors (MR) has been actively pursued by U.S. industry and academia in the 80's and 90's. The potential benefits that result from this reactive separation concept include enhanced productivity and improved energy efficiency for several key reaction processes in the power, chemical and refinery industries. Although the concept has been verified experimentally, existing membranes have failed to be implemented commercially due primarily to their lack of material stability in the application environment. Development of a silicon carbide (SiC) based hydrogen selective membrane is proposed here in this project to overcome this technical barrier. Use of the SiC membrane as an MR can potentially reduce the capital and operating cost of the water-gas-shift reaction (WGS), one of the key reactions for hydrogen production in coal-fired power plants. The SiC membrane is expected to have excellent hydrothermal and chemical stability under the proposed application environment, eliminating material-related problems associated with existing membranes, such as those based upon dense metal, microporous SiO<sub>2</sub>, and their hybrids.

During this project, we have completed development, fabrication, and characterization of macroporous SiC substrates. The hydrogen selective SiC layer was also prepared via a chemical vapor deposition/infiltration technique (CVD/I), sol-gel and calcinations of pre-ceramic polymers. The multilayer composite hydrogen selective SiC membrane thus developed is robust in its structural integrity and efficient in its gas permeation, making it ideal for the proposed high temperature high pressure application.

Specifically macroporous SiC membranes was developed as substrates. Macroporous SiC membranes with pore sizes ranging from 0.1 to >0.2 $\mu$ m were prepared from commercially available SiC powder with selected binders via extrusion and then sintered at >2,000 $^{\circ}$ C. The narrow pore size distribution, nearly Knudsen selectivity, and the uniform top surface are indicative of a high quality, defect free substrate. Meso-/micro-porous SiC thin film with an average pore size of 6 to 40 $\text{\AA}$  have been developed as an intermediate layer. This porous thin film was prepared by coating the above substrate with polycarbosilane as a precursor and subsequent calcination at ~1,400 $^{\circ}$ C. An alternative approach has also been explored with a SiC precursor sol instead of polycarbosilane. Both approaches deliver nearly defect free meso-/micro-porous thin film as evidenced by the surface photomicrograph, permeation characterization and pore size distribution analysis. The unsupported film and membranes were also subjected to treatment at different corrosive and harsh environments, including immersing them in HF, burning in air, and reacting with steam at high temperatures. The effects of these different treatments on the internal surface area, pore size distribution, and transport properties, were studied for both the powders and the membranes using the aforementioned techniques and XPS. The materials are shown to have satisfactory hydrothermal stability.

In parallel the hydrogen selective SiC membranes were deposited on existing commercial ceramic substrates via a CVD/I technique. Triisopropylsilane (TPS) was used as a precursor in our study. The helium permeance ranges from 0.65 to 13.9 m<sup>3</sup>/m<sup>2</sup>-hr-bar with a He/N<sub>2</sub> selectivity of 4 to 85 for the membranes after conversion to SiC at 1,000 $^{\circ}$ C. The wide range of results reflects our evaluation of several key deposition parameters as part of the feasibility study. The SiC membrane prepared at a high temperature (>1,000 $^{\circ}$ C) is expected to be thermally stable at the proposed application temperature (180 to 450 $^{\circ}$ C). In addition the SiC membranes prepared via CVD/I in this study have demonstrated their hydrothermal stability in a nearly 100 hour test at 750 $^{\circ}$ C and at 50% of steam (atmospheric pressure). Helium was used here as a simulant to hydrogen. In addition, high selectivity of H<sub>2</sub> to CO and CH<sub>4</sub> has also been demonstrated.

Building upon the positive progress made in the membrane development study, we conducted an optimization study to develop an optimized H<sub>2</sub> selective membrane with sufficient hydrothermal stability suitable for the WGS environment. In addition, mathematical simulation has been performed to compare the performance of the membrane reactor (MR) vs conventional packed bed reactor for WGS reaction. Our result demonstrates that >99.999% conversion can be accomplished via WGS-MR using the hydrogen selective membrane developed by us. Further, water/CO ratio can be reduced, and >97% hydrogen recovery and <200 ppm CO can be accomplished according to the mathematical simulation. Thus, we believe that the operating economics of WGS can be improved significantly based upon the proposed MR concept. In parallel, gas separations and hydrothermal and long-term-storage stability of the hydrogen selected membrane have been experimentally demonstrated using a pilot-scale tubular membrane under a simulated WGS environment.

In summary this project has demonstrated (i) the technical feasibility of preparing SiC-based H<sub>2</sub> selective membrane via the proposed approaches and (ii) their improved hydrothermal stability. In addition, mathenatril simulations

indicates tremendous benefits can be delivered as a result of the implementation of the WGS-MR using the H<sub>2</sub>-selected membranes developed from this project.

## 2. INTRODUCTION

The U.S. energy industry is undergoing a profound change as a result of legislation in a number of states mandating power generation deregulation and increasingly more stringent environmental standards. For coal-fired power plants to continue to play a significant role in the energy scene and to remain a major source (as they currently are) of electricity production for the world, new advanced coal technologies must be developed. To be competitive the new technologies must exhibit enhanced efficiencies in electricity-from-coal production. They must, furthermore, employ cost-effective environmental compliance solutions, including the removal of the key critical pollutants ( $\text{NO}_x$  and  $\text{SO}_x$ ) and the capability of capturing, concentrating and disposing  $\text{CO}_2$  in a manner that assures closure of the carbon fuel cycle. One aspect of the new promising technologies involves hydrogen production, purification and utilization in the coal-based power plant. Under the concept of co-production in a coal-based power plant (IGCC) [29] this means the development of better hydrogen separation technologies, which can significantly improve production economics and are robust to minimize maintenance requirements and failures. Advanced high temperature hydrogen permselective membrane-based technologies show the greatest promise for non-incremental technology leaps in this area.

A hydrogen selective membrane has been suggested to be used to recover hydrogen from the gasification product at 550 to 1200°C and 15-70 atm. Also, this membrane has been suggested as a catalytic membrane reactor (MR) to enhance hydrogen conversion in a water gas shift reaction (WGS) and then recover hydrogen as a product at 200 to 400°C [21]. In this project, we have focused on the development of an advanced (i.e., SiC-based) hydrogen selective membrane and its use as an MR for WGS reaction. We believe that the SiC membrane can be developed cost effectively by building upon the success and experience we have in the  $\text{SiO}_2$ -based hydrogen selective membrane [24]. Furthermore, the MR-WGS reaction is considered an ideal choice to demonstrate the MR technology due to its moderate operating condition and favorable catalytic reactions. Ultimately, this robust membrane can be used to recover hydrogen from the gasification product and industrial streams.

The key advantages of the SiC membrane are their thermal, hydrothermal and chemical stability which result from two factors:

- Conversion temperature. The conversion temperature (1,000 to 1,400°C) is much higher than the application temperature (300 to 600°C). Hence, the SiC membrane is expected to be stable under these conditions.
- Covalent bonding. The source of the stability is the covalent bonding of the SiC. This compares with ionic bonding that prevails in metal oxide based hydrogen selective membranes. The ionically bonded materials are very susceptible to sintering in the presence of steam at high temperatures. No such problem exists for SiC [23].

Although oxidation of SiC was reported at high temperatures in highly oxidizing environments [20], our proposed application is at lower temperatures, i.e., 300 to 600°C under mildly reducing conditions. Therefore, the proposed SiC membrane is promising for the proposed application.

### 2.1 Project Objectives

The primary objective of this research project has been to demonstrate the feasibility of developing a SiC-based  $\text{H}_2$  permselective membrane suitable for implementing the reactive separation concept, in the water-gas-shift reaction (WGS). Key specific technical objectives are listed as follows:

- development of SiC macro- and meso-porous substrates as support for the SiC hydrogen selective membrane,
- development of the nanoporous SiC membranes using the thin film coating and chemical vapor deposition/infiltration (CVD/I) preparation techniques available to us,
- demonstration of the hydrogen permselectivity over  $\text{CO}$ ,  $\text{CO}_2$ ,  $\text{CH}_4$ , and others relevant to the proposed WGS application.
- evaluation of the hydrothermal/thermal/mechanical stability in the proposed WGS reaction environment, and
- estimation of benefits offered by the reactive separation using the developed hydrogen selective SiC

membranes.

## 2.2 Macro- and Meso-Porous SiC Membranes as Substrates for SiC-H<sub>2</sub> Selective Membranes

Existing ceramic membranes used in the development of M&P's SiO<sub>2</sub> based hydrogen selective membranes (primarily  $\gamma$ -Al<sub>2</sub>O<sub>3</sub> membranes with pore sizes between 40 and 100 Å) may not be suitable as supports for the SiC hydrogen selective membrane for two reasons:

- **Thermal mismatch.** The thermal coefficient of expansion of Al<sub>2</sub>O<sub>3</sub> and SiC are 8.2 and 4.4×10<sup>-6</sup> in/°C, respectively, at 25 to 1,000°C. Hence, it is possible that the thermal mismatch between the  $\gamma$ -Al<sub>2</sub>O<sub>3</sub> substrate and the SiC-H<sub>2</sub> selective thin film over the deposition and operating temperature range (i.e., 400 to possibly >1,200°C) could yield cracking of the membrane.
- **Thermal and hydrothermal stability.** Sintering and pore size growth of the existing 40 to 100 Å  $\gamma$ -Al<sub>2</sub>O<sub>3</sub> membranes at high temperature, particularly in the presence of steam, may be problematic. In general, the 40 Å membrane is suitable for temperatures less than 600°C and the 100 Å for temperatures <1,000°C. These use temperatures are reduced considerably in the presence of low to moderate pressure steam. However, the temperature required to prepare the SiC-H<sub>2</sub> membranes (750 to perhaps 1,400°C) and to operate in the proposed applications (400 to 600°C at moderate steam pressures of 3 to 20 bar) present potential problems for  $\gamma$ -Al<sub>2</sub>O<sub>3</sub> based substrates.

For these reasons a SiC based membrane as a substrate for subsequent deposition of a SiC-H<sub>2</sub> thin film may be necessary. To facilitate the project progress, we took a two-pronged approach: (i) development of a SiC porous membrane as substrate for depositing the SiC H<sub>2</sub> selective membrane layer, and (ii) feasibility test on the use of  $\gamma$ -Al<sub>2</sub>O<sub>3</sub> for depositing SiC thin film specifically for calcination at a low temperature, i.e., near 1,000°C.

## 2.3 Porous SiC Membranes via Prepyrolysis of Pre-Ceramic Polymers

Pre-ceramic polymers are currently attracting growing attention as a means of producing ceramics, particularly non-oxide ceramics. The reason for this renewed interest is that the pre-ceramic polymers can be processed and formed at relatively low temperatures compared to the production of conventional structural ceramics. For the preparation of SiC of H<sub>2</sub> selective membranes via the pyrolysis of pre-ceramic polymers, our rationale is based upon the following:

- Polycarbosilanes (PCS) and polysilanes are two pre-ceramic polymers known to produce silicon carbide upon controlled pyrolysis at high temperatures in the absence of oxygen. Thus it is worthwhile to explore the synthesis of SiC H<sub>2</sub> selective membrane using pre-ceramic polymers as an alternative to the CVD/I technology.
- The organometallic to inorganic (mineral) conversion occurs mostly in the temperature range between 500 to 800 °C. Nucleation and crystallization processes occur in the temperature range between 800 to 1000 °C along with the formation of nanosize crystalline SiC. Since the appearance of the crystalline phase is accompanied by the disappearance of the amorphous material, the presence of such a crystalline phase may not be beneficial for the preparation of microporous SiC membranes for the H<sub>2</sub> separation. On the other hand, crystalline SiC is known to have a higher corrosion and oxidation resistance and mechanical strength than amorphous SiC. Consequently, one expects that an optimal pyrolysis temperature may exist which produces membranes with an acceptable separation factor and sufficient mechanical and thermal resistance for the proposed separation.

Thus, an empirical approach has been taken in this project to identify an optimum condition to develop a SiC membrane qualified for our application.

## 2.4 H<sub>2</sub> Selective SiC Membranes via Chemical Vapor Deposition/Infiltration (CVD/I)

The CVD/I approach has been proposed as a route to H<sub>2</sub> selective SiC membranes for several reasons:

- Highly permselective H<sub>2</sub>-selective silicon oxide (SiO<sub>2</sub>) membranes [31] and the necessary CVD/I hardware [24] were developed previously by Media and Process Technology Inc. (M&P). Although this SiO<sub>2</sub> membrane shows limited hydrothermal stability, the CVD/I technique coupled with the selection of a proper precursor and deposition conditions can be used to develop a H<sub>2</sub>-selective SiC membrane.
- One literature study [27] presents the deposition of a thin SiC film via CVD/I using triisopropylsilane (TPS) as a precursor. Although the membrane selectivity for H<sub>2</sub> & He over N<sub>2</sub> was no better than Knudsen separation, the deposition and formation of a true SiC film on a microporous substrate via a CVD/I approach was confirmed based upon XPS analysis. Another literature study confirms the presence of SiC under a similar preparation condition [26].

Morooka, *et al.*[27] prepared SiC membranes by chemical vapor deposition on  $\gamma$ -alumina substrates at 700-800 °C using tri-isopropylsilane as the precursor. After the deposition process, the membranes are heat-treated in argon at 1000 °C for 1 h. The resulting membranes are tested for the separation of H<sub>2</sub>/H<sub>2</sub>O mixtures. The permeation experiments are performed at temperatures between 200°C and 400°C, and have shown a H<sub>2</sub>/H<sub>2</sub>O selectivity in the range of 3-5.[27] SiC membranes were prepared by chemical vapor infiltration (CVI) into  $\gamma$ -Al<sub>2</sub>O<sub>3</sub>-coated porous  $\alpha$ -Al<sub>2</sub>O<sub>3</sub> tubes by Takeda *et al.*[28] The gases utilized were SiH<sub>2</sub>Cl<sub>2</sub> and C<sub>2</sub>H<sub>2</sub> diluted with hydrogen. They were supplied alternatively to the porous tube during heating at 800-900 °C. The produced SiC membrane showed hydrogen permeances in the range of  $1 \times 10^{-8}$  mol.m<sup>2</sup>.s<sup>-1</sup>.Pa<sup>-1</sup> with a H<sub>2</sub>/N<sub>2</sub> selectivity of 3.36 at 350 °C. Using  $\gamma$ -alumina as the support for the preparation of silicon carbide membranes presents a number of challenges for the type of applications these membranes may be useful for. Porous  $\gamma$ -alumina is not very resistant to corrosive environments. In addition, its thermal expansion coefficient is different from that of silicon carbide, raising concerns about the mechanical stability of the resulting composite membrane system. Lee and Tsai [29] have prepared asymmetric SiC membranes by low-pressure chemical vapor deposition (LPCVD) of SiH<sub>4</sub>, C<sub>2</sub>H<sub>2</sub> and argon mixtures at 800 °C on the surface of Al<sub>2</sub>O<sub>3</sub>-doped SiC macroporous supports. The macroporous SiC support, itself, had an asymmetric structure, i.e., the alumina content decreased from the center to the surface of the support. The CVD process reduced the pore size of the membrane from 297 nm to 14 nm.[29] However, this pore size reduction is achieved at the cost of a large reduction in the permeance of the membranes.

In spite of the mediocre selectivity obtained from the literature study, we believed that our prior experience in CVD of SiO<sub>2</sub> can overcome these difficulties. Our proposed SiC CVD/I technique allows us to maximize hydrogen permeance and selectivity by removing excess unreacted, deposited carbon. This offers a direct and controllable technique to develop a high performance SiC membrane.

## 2.5 Microporous SiC Membranes via Sol-Gel Approach

In this project we also pursued the preparation of asymmetric SiC membranes using a sol-gel method. In our study we have utilized a number of commercial silica sols with different sol particle sizes. These are used as the silicon source for production of SiC. Phenolic resin is utilized as the carbon source. The SiC sol precursors are then coated on the SiC substrates, which are prepared by our group [30] using dry-pressing techniques, and sintering at 1950°C. The SiC sol precursors undergo carbothermal reduction at high temperatures to produce the final SiC thin films. The sol-gel step is an important intermediate stage in the preparation of asymmetric microporous SiC membranes (the final stage can be a CVD/CVI or a polymeric precursor pyrolysis step), which are capable of withstanding high service temperatures and are thermally stable to the presence of steam. These sol-gel membranes, in addition, can potentially find application in nano- and ultrafiltration applications of corrosive liquid mixtures.

We are not aware of other studies, which report on the use of a sol-gel technique for the preparation of SiC membranes. A number of prior studies in recent years have, however, focused on the preparation of SiC powders using sol-gel techniques. Cerovic *et al.*, [12] for example, have prepared silicon carbide powders by heating a mixture of a silica sol, prepared by an ion exchange method, with saccharose or activated carbon (as the carbon sources), and boric acid; the latter is reported to act as the catalyst for the carbothermal reduction of silica with carbon at 1550°C. They report that the optimum molar ratio of C/Si for the production of SiC is 3 for activated carbon and 4 for saccharose. The diameter of the spherical SiC particles prepared with activated carbon was twice that of the particles prepared from saccharose. Using phenyltrimethoxysilane (PTMS), and/or tetraethylorthosilicate (TEOS) as the silica source Seog and Kim [13] have prepared silicon carbide powders, which are made of spherical particles. Mono-dispersed spherical powders were produced using a base catalyzed route, while poly-dispersed powders were obtained with the aid of an acid-base catalyzed route. A number of different carbon sources such as

ethylcellulose, polyacrylonitrile (PAN), and starch were utilized by Raman *et al.* [14] for reaction with a silicon source at 1550°C to produce SiC powders. It was shown that the type of carbon source utilized determines the crystalline form of SiC that is produced and the grain size.

## 2.6 Product Development and Process Simulation for WGS

In the last year of the project, we focused on the product development specific for hydrogen recovery from coal gasifier off-gas via WGS. Our approach includes:

- ❑ Perform mathematical simulation for WGS shift reaction to determine benefit potentially delivered by the hydrogen selective membrane developed up to this point.
- ❑ Conduct membrane characterization relevant to the proposed WGS reaction environment identified by mathematical simulation.
- ❑ Verify hydrogen recovery via the selected hydrogen selective membrane using a pilot scale unit.

Based upon the above fundamentals and relevant literature studies, experimental procedures for the techniques proposed were designed and are presented in the next section:

## 3. EXPERIMENTAL PROCEDURE

### 3.1 Macroporous SiC Membranes as Substrates for SiC-H<sub>2</sub> Selective Membranes

In this project, macroporous ceramic carbon substrate in a disk configuration was prepared by conventional extrusion technology using commercial SiC powder as the starting material. Then the disk was fired at >2,000°C to form SiC macroporous substrate. XRD, pore size distribution analysis and gas permeation were performed to characterize the resultant substrates. Please refer to the publication in Appendix for details of experimental procedure.

### 3.2 H<sub>2</sub> Selective SiC Membranes via Chemical Vapor Deposition/Infiltration (CVD/I)

An unsupported SiC film (i.e., powder) was prepared via CVD/I using TPS as a precursor. This unsupported film was used to expedite the characterization of the resultant SiC. Briefly, the protocol involved (i) deposition at 750°C in helium to form a thin film and (ii) calcination at 1,000 to 1,400°C to convert the deposit into SiC. Following a similar protocol, we applied the proposed CVD/I technique on the Al<sub>2</sub>O<sub>3</sub> substrate<sup>1</sup> (i.e., 100Å) at 750°C until the helium/nitrogen selectivity was maximized. This CVD/I treated substrate was subsequently calcined at 1,000°C for two hours for conversion to SiC. Details of the preparation procedure are described in the publication listed in the Appendix.

### 3.3 H<sub>2</sub> Selective SiC Membranes via Pyrolysis of Pre-ceramic Polymers

Unsupported SiC ceramic thin film was prepared from allylhydridopolycarbosilane (AHPCS) and hydridopolycarbosilane (HPCS) (kindly provided to us by Starfire Systems). After pyrolysis and calcination, the powder was then characterized with XRD and pore size distribution (BET method). The results were then used to select an optimum pyrolysis and calcination condition for preparing a supported SiC membrane from the pre-ceramic polymers. H<sub>2</sub>-selective SiC microporous membranes were prepared by coating AHPCS on the SiC substrate prepared (pore size in the range of ~300Å) following pyrolysis at a selected temperature of 600°C. Multiple coating/pyrolysis is applied to reach a desirable separation efficiency.

---

<sup>1</sup>40Å  $\gamma$ -Al<sub>2</sub>O<sub>3</sub> membrane was pre-calcined at 1000°C to insure its thermal stability at this temperature for CVD/I and calcination. The resultant pore size is estimated ~100Å.

### 3.4 Microporous Membranes via Sol Gel Approach

#### 3.4.1 Sol-gel Synthesis of Silicon Carbide

A variety of silica sols (both water and alcohol based) have been utilized in the investigation. For the materials, whose preparation is described here, a particular organo-silica sol type IPAST, with a particle size in the range of 8-10 nm (see Fig. 1) is used as the silica source, as received from the manufacturer (Nissan Chemical Industries, Ltd). A phenolic resole type resin (Occidental Chemical) is used as the carbon source. A 50 wt % solution of phenolic resin in ethanol is mixed with the silica sol in a quantity that is adjusted to obtain a molar ratio of Si/C =1:3. The choice of this Si/C molar ratio is based on the stoichiometric requirement for the completion of the overall carbothermal reduction reaction, which is thought to proceed as follows [15]:



The mixture of silica sol and phenolic resin is then sonicated using an ultrasonic device for 10 min in order to obtain a homogeneous gel-polymer mixture. Subsequently, the procedure one follows depends on whether one prepares powders or membranes. For the powders, the sample is dried at room temperature overnight and then transferred into an alumina crucible. The crucible containing the dried gel is then placed in a tubular furnace. The samples are heated first up to 800°C with a heating rate of 75°C/h and then up to 1550 °C with a heating rate of 50°C/h. The gel is calcined at 1550°C for 3 h; upon calcination it is then cooled down to room temperature at a rate of 85°C/h. During the calcination process the sample is constantly purged with ultra-high purity argon. The membrane preparation is described below.

#### 3.4.2 Membrane Preparation Using the Sol-Gel Method

The supported SiC sol-gel membranes are prepared utilizing macroporous SiC substrates. These substrates are prepared as follows.[11] A silicon carbide fine powder (Sumitomo Osaka Cements, Japan) with an average particle size of 0.03µ is mixed with a more course silicon carbide powder (Superior Graphite Co.,) with an average particle size of 0.6µ in the ratio of 1:2. Boron carbide (in the amount of 0.1 wt %) and phenolic resin (in the amount 4 wt %) are used as the sintering aids. The mixture of powders and various sintering aids are pressed into disks, which are then calcined at 1950°C to obtain the macroporous SiC membrane substrates (more details about the preparation of such substrates can be found in our prior publication)[11]. These SiC substrates are then used for further surface modification via the sol-gel technique.

The silicon carbide membranes are prepared by conventional dip-coating techniques. One first prepares the solution containing the appropriate amounts of the silica and carbon sources and sonicates it for 10 min in order to obtain a homogeneous blend. The macroporous SiC substrate to be dip-coated is wrapped with Teflon tape on one side, and is dipped in the sol solution for a period 30 s; it is then withdrawn out of the solution with a withdrawal rate of 0.001m/s. After the coating process is completed, the coated substrate disk is placed in an alumina crucible and is then inserted in the tubular furnace. The sample is heated to 1550°C with a heating rate of 50°C/h, where it is calcined for 3 h under an argon atmosphere; upon calcination it is cooled to room temperature with a cooling rate of 50°C/h. If additional coatings are required they are applied after the first calcination step using the same dip-coating/calcination procedure.

#### 3.4.3 Characterization of SiC Membranes

The permeation characteristics of the membrane are measured using argon and helium as the test gases. The transport properties of each membrane are reported in terms of the permeance of the two individual gases and the ideal separation factor (defined as the ratio of permeances of these two gases). The absolute values of permeance and the separation factor are both important in terms of determining the usefulness of the membrane for further applications and processing. The permeance of each species is measured using a laboratory permeation apparatus, which has been described elsewhere[11]. Briefly the membrane disk is placed in between the two half-cells of the apparatus, one chamber is pressurized at the required pressure, while the other is maintained at

atmospheric pressures. The flow rate of gas exiting the lower pressure chamber  $Q_i$  ( $\text{m}^3/\text{s}$ ) is measured using a soap-bubble flow meter. Since the thickness of the thin layer is not precisely known the permeance (instead of the permeability) of each gas  $K_i$  in  $\text{m}^3/(\text{m}^2 \text{ Pa s})$  is calculated from the following equation.

$$K_i = Q_i / (A \Delta P_i) \quad , \quad (2)$$

where  $A$  is the cross-sectional area ( $\text{m}^2$ ), and  $\Delta P_i$  is the pressure difference that exists across the membrane disk (Pa). The separation factor between He and Ar, as noted previously, is defined as the ratio of their permeances calculated from equation (2). If the sol-gel membrane has no substantial number of macroporous defects being present, one expects this ratio to be equal to the Knudsen separation factor ( $S_k$ ) given (for the case of the He and Ar pairs) by the following relationship.

$$S_k = \sqrt{\frac{MW_{Ar}}{MW_{He}}} \quad (3)$$

where the  $MW_i$ 's are the molecular weights of the two permeating gases.

For both the powders and the membranes X-ray diffraction (XRD) analysis is used in order to identify the crystalline compounds that are present. The XRD technique is complemented with X-ray photoelectron spectroscopy (XPS) measurements, which determine the surface composition of the materials. XPS can potentially identify amorphous compounds, which may not be detected by XRD. The pore size distributions of both powders and films are measured using an ASAP2010 (Micromeritics) BET apparatus. For BET data analysis we utilize the BJH and Horvath-Kawazoe models. Therefore, the pore size distributions (PSD) generated must only be viewed as qualitative measures of the pore structure (two SiC membranes with the same PSD's are likely to have the same pore structure characteristics) rather than as quantitative indicators of the pore size. Scanning electron microscopy (SEM) and atomic force microscopy (AFM) are also used to study the surface morphology of the membranes. The SEM technique is used to locate the position of the film, and in order to determine the degree of its adhesion to the underlying macroporous substrate. AFM is utilized to determine the degree of surface roughness, which is important when determining whether these materials are appropriate as substrates for the further deposition of microporous films by other techniques.

### 3.5 Thermal and Hydrothermal Stability Test

Two approaches were pursued to evaluate the thermal and hydrothermal stability of the SiC membrane. They are discussed as follows:

- The SiC unsupported thin film prepared from sol-gel technique was used to study the thermal and hydrothermal stability of the SiC membrane. Use of the unsupported film allows us to reliably measure the pore size change before and after the hydrothermal stability test because the measurement is not diluted by the bulk inert substrate. Since the sol-gel prepared SiC membrane with a larger pore size (e.g., 6 to 12Å) does not deliver any hydrogen separation. This sol-gel prepared membrane is and will be used as a substrate only. Thus, the hydrothermal stability test of the sol-gel prepared unsupported thin film will provide background information on the stability of the support, not the H<sub>2</sub> selective membrane.
- Under the second approach, we use the CVD/I prepared SiC H<sub>2</sub> selective membrane for the hydrothermal stability test. Since the bulk substrate contributes to majority of the sample weight, gas permeation, instead of surface area measurement, was used to infer the structure change under the selected hydrothermal condition.

The hydrothermal test selected in this study covers the temperature ranging from 300 to 750°C and the 50% steam at ambient pressure. The temperature range selected is consistent with the condition currently employed by the WGS reaction. The steam partial pressure is much lower than the actual pressure in the WGS reaction environment; however, it is a good starting point to screen the hydrothermal stability of the SiC membranes.

## 4. RESULTS AND DISCUSSIONS

#### 4.1 SiC Macro- and Meso-porous Membranes as Substrates

Macroporous SiC membranes with pore sizes ranging from 0.1 to >0.2 $\mu$ m have been developed successfully with consistent quality. The membranes were prepared from commercially available SiC powder with selected binders and then sintered at >2,000°C. Characterization data is presented for a typical membrane (Sample ID: P1). Figure 1 shows the pore size distribution of the resultant membrane and the particle size distribution of the starting powder. Figure 2 shows the helium and nitrogen permeance and selectivity (ratio of the He and N<sub>2</sub> permeance). Figure 3 shows an SEM photomicrographs of the top surface. The narrow pore size distribution, nearly Knudsen selectivity at low pressure, and the uniform top surface are indicative of a high quality, defect free substrate which is ideal for subsequent deposition of a mesoporous thin film. In summary, microporous SiC substrates have been fabricated for subsequent deposition of SiC thin films. The effect of binders on the porosity and pore size distribution of the macroporous SiC membranes has also been systematically studied, which is summarized in a paper published in I&EC Research [11] (see Appendices).

Mesoporous membranes with an average pore size of ~40Å have been developed via deposition of a SiC thin film on the macroporous SiC substrates described above. Using a polycarbosilane (PCS) as a precursor with subsequent calcination at ~1,400°C, we have successfully deposited a SiC mesoporous film on the macroporous substrate. Figure 4 shows the pore size distribution (BET measurement) which ranges from ~10 to 80Å. Figure 5 shows an XRD pattern that confirms full conversion to SiC from this polymer precursor. The SEM photomicrograph of this microporous SiC membrane is presented in Figure 6. After calcination, the top surface is a smooth and defect-free mesoporous SiC film. He and N<sub>2</sub> gas permeances at room temperature are shown in Table 1. Slightly better than Knudsen separation at room temperature was obtained (2.90 to 3.25 vs 2.65), supporting the presence of extremely small pore sizes, e.g., ~10 to 20Å. We believe that the mesoporous SiC membrane developed from the selected polymer is sufficient as a substrate for developing a SiC-H<sub>2</sub> selective membrane via CVD/I discussed in Sec. 3.2. Under this project, we successfully demonstrated the feasibility of preparing mesoporous SiC substrates as evidenced by the surface photomicrograph, permeation characterization and pore size distribution analysis. The fabrication procedure developed here will be one of the two methods to be selected in the future to prepare SiC based mesoporous membranes to be used as supports for further development of the SiC-based H<sub>2</sub> selective membrane via CVD/I. The other method is through the sol-gel technique as described in sec. 3.4.

Mesoporous membranes with an average pore size of 6 to 12 Å have been developed via coating of SiC precursor gel on the macroporous SiC substrates described above. Synthesis of silicon carbide powders and thin films via sol-gel involves combining a silica sol with a carbon source, followed by the further carbothermal processing of the resulting mixture at high temperatures. A number of different silica sols are used in our experiments as the silica source. In this report only the thin film prepared from Sol #2 (8 to 11 nm in size with 30% concentration) is presented. We have also deposited the thin film on silicon carbide disk substrates which have an average pore size distribution 0.3-0.5  $\mu$ m X-ray diffraction result for the sol-gel silicon carbide powder samples is shown in Figure 7. All the peaks in this figure correspond to  $\beta$ -silicon carbide, which indicates that no other crystalline phases are present. Using the N<sub>2</sub> adsorption-desorption technique we have also measured the pore volume and pore-size distribution of all the SiC powder samples are shown in Figure 8. Atomic force microscopy (AFM) was used to study the surface morphology of the sol-gel coated samples. Figure 9 shows the AFM image of the SiC membrane prepared via sol-gel technique. There are no cracks and/or pinholes observed in the membrane layer and the surface appears to be relatively smooth. The results of the permeation test are shown in Figure 10. The ideal separation factor estimated from the He and N<sub>2</sub> permeances is close to the ideal selectivity based upon Knudsen diffusion (He/N<sub>2</sub>), as compared with the original substrate, which provided no separation at all (separation factor =1).

#### 4.2 H<sub>2</sub> Selective SiC Membranes via Chemical Vapor Deposition/Infiltration (CVD/I)

An unsupported SiC film (i.e., powder) was successfully produced via the CVD/I protocol developed in-house using TPS as a precursor. Figure 18 confirms the formation of SiC according to the XRD analysis of the produced unsupported film. Crystalline SiC peaks are evident in the samples calcined at 1,200 and 1,400°C. Although the sample calcined at 1,000°C did not exhibit SiC peaks, it is believed that amorphous SiC is present at this temperature indicated by the peak at the low angle end. Literature studies using the same precursor confirm the formation of SiC at 1,000°C [6, 8] based upon XPS analysis. In addition, the XRD analysis shows excess unreacted (not incorporated into the SiC) crystalline carbon is present in the sample calcined at 1,200°C. The disappearance of this peak at

1,400°C suggests that additional SiC is formed. From this study, it was concluded that (i) SiC formation occurs at 1,000 to 1,400°C; (ii) higher calcination temperatures,  $T_c$ , yield higher degrees of SiC crystallinity; and (iii) unreacted carbon residue is present at <1,400°C with the selected precursor and protocol. In summary, the feasibility of forming a SiC film via the CVD/I technique has been clearly demonstrated here.

SiC hydrogen selective nanoporous membranes following the above CVD/I protocol and using the selected precursor (i.e., TPS) have been successfully prepared using M&P's  $Al_2O_3$  membranes as substrates. An SEM photomicrograph of the cross section of the SiC membrane is shown in Figure 19a and b. Since no deposition of an additional layer on top of the support is indicated, deposition of the SiC occurs inside the top layer of the support. According to our previous experience with  $SiO_2$   $H_2$  selective membranes, an extremely thin film was deposited, estimated at less than 1.5 $\mu m$  based upon EDAX mapping of our earlier  $SiO_2$  membranes. Further, this black SiC film remained visibly intact after oxidation in air at 400°C for two hours, indicating that a thin SiC film was prepared on the white  $Al_2O_3$  substrate. An SEM photomicrograph of the oxidized SiC membrane is presented in Figure 20. In summary, SiC formation via the CVD/I technique was confirmed and has been successfully deposited as a thin film on a mesoporous support with the selected precursor.

The helium<sup>2</sup> permeance ranges from 0.65 to 13.9  $m^3/m^2/hr/bar$  with a He/ $N_2$  selectivity of 4 to 85 for the membranes after conversion to SiC at 1,000°C. Table 2 summarizes the results from these membranes (total of 12 samples). Figure 21 presents permeance vs. temperature for one of the membranes. Helium permeance increases significantly with temperature, indicative of activated diffusion, whereas the nitrogen permeance decreases with temperature, indicative of Knudsen flow for this penetrant. This phenomenon is consistent with our previous experience with  $SiO_2$  hydrogen selective membranes. The wide range of results shown in Table 2 reflects our evaluation of several key deposition parameters as part of the feasibility study. Good reproducibility<sup>3</sup> of the CVD/I technique was demonstrated in our previous study with the  $SiO_2$  membrane. As a general trend, conversion to SiC at 1,000°C does not drastically alter the permeance and selectivity of the membrane deposited at 750°C. This phenomenon is expected because the SiC calcined at this temperature is very amorphous (see Figure 18). This trend offers us an unique and practical fabrication method, i.e., developing a high quality SiC membrane via on-line monitoring of the membrane permeance during deposition. From the results of this feasibility study it was concluded that (i) nanoporous SiC membranes suitable for high temperature hydrogen separations could be developed and (ii) on-line monitoring of the progress of the CVD/I deposition is feasible and practical to optimize the membrane synthesis in a reproducible manner. The degree of crystallinity generated in this temperature range (see Figure 18) may play a significant role in shifting the permeance vs. temperature relationship, which can be tailored to deliver a membrane for a given application temperature.

High selectivities of He to  $CO_2$  and  $CH_4$  have also been demonstrated. The selectivities of He/ $CO_2$  and He/ $CH_4$  are 83.4 and 39.4, respectively, for membrane TPS-021 at 750°C. The He/ $N_2$  selectivity is 76.1 for this membrane at this temperature. The rejection of  $CO_2$  and  $CH_4$  are similar to  $N_2$  so that He/ $N_2$  represents a good surrogate gas mixture for evaluating this membrane. Table 3 lists the permeance vs. temperature up to 1,000°C for several samples prepared under this project. Evidently, some of the samples demonstrate an excellent selectivity at a higher temperature, i.e., >600°C; while others show the selectivities even at a lower temperature i.e., 800°C. It is believed that the pore size distribution plays a significant role in determining its permeance vs. temperature behavior. To achieve an excellent selectivity at a lower temperature, e.g., 300-600°C, a larger pore size is essential.

The presence of excess carbon in the SiC membrane was verified via XRD as shown in Figure 18. The removal of this excess carbon has been proven to be a useful tool to enhance the permeance of the membrane. Steam was introduced with the objective of removing excess carbon via carbon-steam gasification from the thin SiC porous film. The resultant membrane after this treatment showed enhanced He permeance as depicted in Figure 22. Steam treatment at 750°C increases the He permeance about 5-fold in this case. Furthermore, this enhanced permeance was shown to be sustainable at one of the proposed application conditions, specifically in the presence of ca. ~50% of steam at 450°C. In summary, the removal of excess carbon has been demonstrated to be a useful tool for enhancing the micro porosity of the SiC membrane. In the future, we plan to investigate various Si to C ratios

---

<sup>2</sup> He was used as a simulate mixture to hydrogen. Our past experience has verified the validity of this simulate mixture for the microporous  $H_2$  selective ceramic membrane.

<sup>3</sup>  $H_2$  permeance of  $7.58 \pm 0.6 m^3/m^2/hr/bar$  (at 600°C) with 95% confidence.

through proper selection of the precursor to derive an optimized protocol for forming a hydrogen selective SiC membrane.

According to our past experience with the SiO<sub>2</sub> hydrogen selective membrane, thermal stability of thin films produced via CVD/I is in general excellent [12]. The SiC membrane prepared at a much higher temperature (>1,000°C) is expected to be thermally stable at the proposed application temperature (300 to 750°C). Therefore only very brief, about 20 hours, experimental work was conducted to demonstrate its stability. Since the SiC membrane has demonstrated the hydrothermal stability (see below), its thermal stability is considered given. No additional work was conducted in this specific area.

The SiC membranes prepared in this study have demonstrated their hydrothermal stability. Figure 25a indicates that the SiC membrane is stable during a nearly 100 hour test of the hydrothermal stability at 750°C and at 50% of steam (atmospheric pressure base). As a comparison, the SiO<sub>2</sub> membrane prepared via CVD/I lost ca. 60% of its permeance in the first few hours of a similar test at a much lower temperature (600°C) and steam pressure (20%) as shown in Figure 25b. In addition, the permeance enhancement obtained by the removal of excess carbon was also demonstrated in a short test to be stable in the presence of steam as shown in Figure 21. Clearly, the SiC membrane displays a much improved hydrothermal stability over the SiO<sub>2</sub>-based hydrogen selective membrane.

### **4.3 H<sub>2</sub> Selective SiC Membranes via Pyrolysis of Pre-ceramic Polymers**

H<sub>2</sub> selective ceramic membranes were prepared from pyrolysis of AHPCS and HPCS. In this report, we focus on the result from the former polymer. X-ray diffraction patterns of the ceramic powders resulting from the pyrolysis of AHPCS2 at different temperatures (i.e., 1,000 to 1,600°C is shown in Figure 11. For the sample produced at 1600°C the spectrum completely agrees with the Powder Diffraction File for SiC. At lower pyrolysis temperatures the XRD spectra are very noisy, potentially signifying the presence of amorphous SiC which crystallizes at higher temperatures. As the temperature increase the amorphous SiC converts into crystalline SiC. The size of the SiC crystallites calculated from the diffraction peak widths by the Scherrer's equation is presented in Figure 12, showing that the crystal grows significantly from ~20 to >100° through calcination from 1,000 to 1,600°C. The powder study confirms that (i) the formation of SiC after pyrolysis of the selected pre-ceramic polymer, and (ii) SiC crystal increases along with the temperature increase. These results suggest that the pyrolysis in the neighborhood of 600 to 1,000°C may be a good starting point for us to identify the optimum pyrolysis temperature for the formation of a hydrogen-selective SiC membrane.

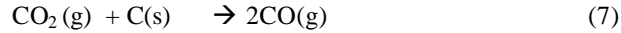
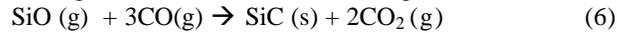
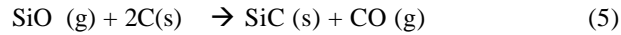
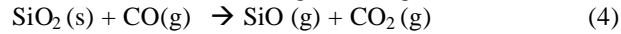
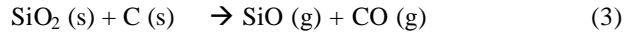
H<sub>2</sub>-selective microporous membranes were prepared with multiple coating/pyrolysis of AHPCS in order to reach a desirable separation efficiency, i.e., >20 for H<sub>2</sub>/N<sub>2</sub> at 200°C. The permeation characteristics (at room temperature) vs the number of coatings are shown in Figure 13. As the number of coatings increases the permeances for both He and N<sub>2</sub> decrease; however, the separation factor remains unchanged and close to the Knudsen regime. Until the fifth coating the separation factor increases to over 3.5, signifying that the membrane has molecular sieving properties. The pre-ceramic polymer selected in this study generates a porous structure of ~5° under the proposed pyrolysis temperature (i.e., 600°C) as shown in Figure 14a. Additional layers of coating primarily minimizes the defects as shown in Figures 14 and 15. The permeation characteristics of the same membrane at higher temperatures are shown in Figures 16 and 17. Note that as the temperature increases the nitrogen permeance decreases (as one would expect from Knudsen diffusion through cracks and pinholes). The He permeation, however, shows an activated type diffusion with permeance increase along with the temperature increase, typical of the behavior observed in other amorphous membranes, SiO<sub>2</sub> microporous membranes. In summary we have successfully developed the SiC hydrogen selective membrane using the pre-ceramic polymer as a precursor. Whether the selection of 600°C is sufficient to deliver a membrane material with a satisfactory hydrothermal stability remains to be evaluated.

### **4.4 Microporous Membrane via Sol-Gel Approach**

#### **4.4.1. The SiC Powders**

Sol-gel production of silicon carbide involves the reaction between silica and a carbon source at relatively high temperatures. This calcination formation process is also called the carbothermal reduction reaction. This is

because during the process silica is reduced (loses its oxygen) by a series of reactions, and is eventually converted to silicon carbide. The carbothermal reaction and the formation of silicon carbide can be easily traced using X-ray diffraction analysis. The bottom line in Fig. 28, for example, shows the XRD pattern of a silicon carbide powder prepared by us by the sol-gel method previously described and after the calcination process. The XRD pattern indicates that the carbothermal reduction reaction has resulted in a material, which is pure silicon carbide, its peaks corresponding to that of crystalline  $\beta$ -SiC. The following set of reactions have been reported to occur during the carbothermal reduction reaction [16, 17]:

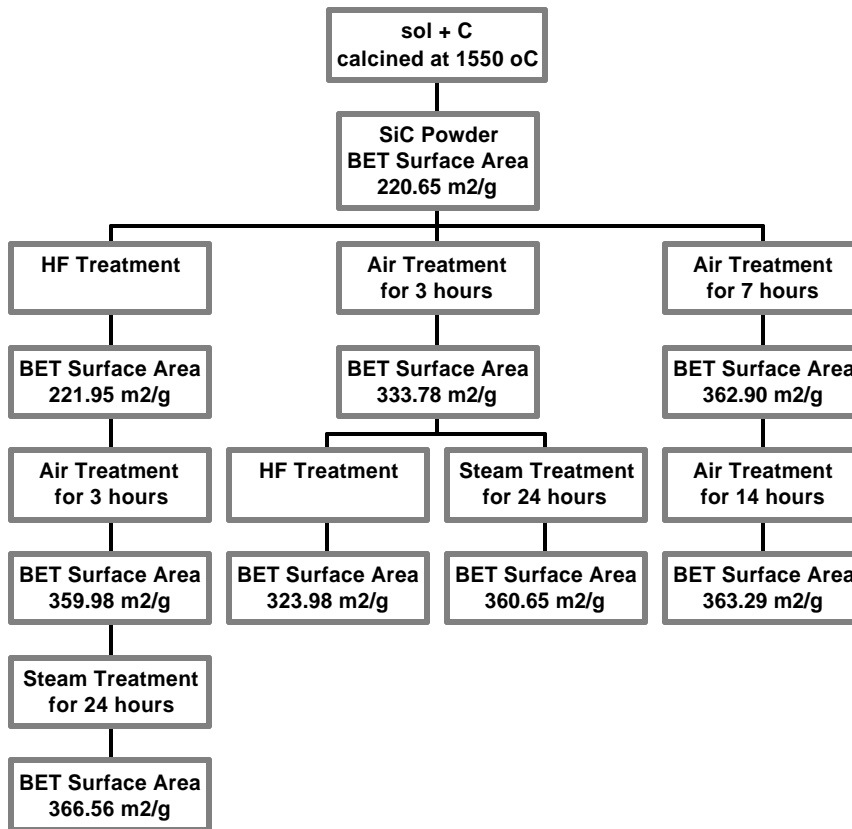


Here (s) and (g) refer to solid and gaseous states, respectively. The main reactions for the formation of SiC are reactions (3) and (5). Reaction (3) occurs rapidly at high temperatures; the SiO(g) that is produced reacts with C(s) that is in close proximity and forms SiC(s). When enough CO and CO<sub>2</sub> are present reactions (4), (6), and (7) may also occur. It is clear from the above mechanism that the miscibility of the carbon source (e.g., the phenolic resin solution) with the silica sol plays an important role in the formation of the final SiC microstructure. The silica sol and phenolic resin need to be homogeneously and well mixed with each other in order for the SiO<sub>2</sub> and C to be in intimate contact and for crystalline SiC to be produced.

Though  $\beta$ -SiC appears to be the form of SiC that forms immediately after the carbothermal reaction treatment of such powders under various conditions may convert this form of SiC into other forms. As can be seen in Fig. 28 treatment of the powder in flowing air at 420°C for 3 h leaves the  $\beta$ -SiC phase unchanged. Treatment in a strong hydrofluoric acid (HF) solution (Aldrich, 40 wt% HF) for 5 h also seems to have a minor effect on the SiC powders. Treatment in a flowing mixture of 50-mol% water and 50-mol% argon at 350°C for 24 h (after it had been treated in air at 420°C for 3 h) seems to convert part of the  $\beta$ -SiC into  $\alpha$ -SiC (see top of Fig. 28). Bootsman *et al.*[18] have studied the phase transformation of different SiC phases. They concluded, in agreement with our own observations, that the 6H ( $\alpha$ -SiC) type is generally the most stable phase. However, whether the other crystal polytypes (including  $\beta$ -SiC) convert into  $\alpha$ -SiC depends on the type and pressure of the atmosphere that prevails, and the type and amount of dopants and impurities that are present in the sample.

To understand the nature of the materials that are formed by the sol-gel technique, and in order to evaluate their performance in corrosive and oxidative environments the as prepared powder samples were subjected to further tests. Three different types of treatments were applied in various sequences. They include heating of the silicon carbide samples in air at 420°C for varying periods of time in order to burn away any unreacted carbon; washing in a strong HF solution (Aldrich, 40 wt% HF), which has been reported by other investigators to etch away any residual silica that may be left behind from the carbothermal reduction reaction[19], and subjecting the samples to a treatment at 350 °C in flowing ultra high purity argon containing 50% mole of steam for a pre-determined period of time, a hydrothermal stability test which is important in terms of the eventual application of such membranes. Table above shows a number of different sequences of tests performed on the sol-gel SiC samples in order to study the effect of each step individually and in combination. We have taken the internal surface area of the powder samples (as measured by BET) as an indicator of the changes in the pore structure brought upon by the various treatments.

The surface areas of SiC samples after various treatments are listed below:



It is clear from the results shown in the table above that etching with HF does not affect the internal surface area of the SiC sample significantly. This is true for the as received samples (less than a 0.6 % change) and the samples after they have been subjected to a 3 h oxidation treatment in air (less than a 3% change). This result taken together with the XRD analysis results of the same sample, which show no evidence for the presence of SiO<sub>2</sub>, confirms that no significant amounts of residual silica are left in the samples after the carbothermal reduction reaction. The fact that the sample that is oxidized in air before the HF treatment, shows a slightly higher change in the surface area may be due to the fact that the HF is removing the passive oxide layer that may form as the result of burning the sample in air.

The BET test results indicate that the surface area of the SiC samples increases considerably after the air treatment at 420 °C for 3 h. This is likely to be due to the burning away of some of the carbon left behind after the calcination process. That little, if any, residual SiO<sub>2</sub> is present and that carbon is left behind after the calcination process may be indicative that the other reactions (4, 6, and 7), in addition to (3) and (5), participate in the formation of SiC. The excess carbon that is left behind may also be an indicator of some loss of volatile Si components (e.g., SiO), which are created at the beginning of the carbothermal reduction process by solid-solid reactions at the interface between silica and carbon. Based on the proposed reaction mechanism, it is likely that the carbon matrix formed by the pyrolysis of the phenolic resin, strongly influences the final silicon carbide structure. Homogeneous mixing of the original precursors, as stated earlier, is essential in order to assure that a final SiC sample is formed, which has uniform properties including porosity and pore structure. The size and type of the silica sols one uses determines the ability of homogeneously distributing the sol with the carbon source. The finer the initial silica sol particles are, for example, the more homogeneously they distribute in the phenolic resin, and actively participate in the carbothermal reaction.

It should also be noted after a certain period of air treatment the surface area does not change significantly (note, for example, the surface areas after the 7 and 14 h treatments in air in column 3 of the table above) indicative that most carbon inclusions are removed in the first few hours of burning in air; further heating in air does not appear to change the properties of the silicon carbide, and the sample appears to be stable.

Steam treatment is equally effective with air oxidation in removing the residual carbon. Note, furthermore, that after the carbon has been removed with air oxidation steam treatment has little effect on the surface area (compare the two values at the bottom of columns 1 and 4 in the table above, which are more or less the same). In terms of the surface area but also of the pore size distribution (see Fig. 29) steam treatment does not affect the structure of the SiC powder after the residual carbon is removed. On the other hand, as shown in Fig. 28, the steam treatment seems to convert some of the  $\alpha$ -SiC into  $\beta$ -SiC; surface area and pore size distribution (see below) appear not to be sensitive indicators of this change, however. Interestingly, steam, HF, and air treatments all have little effect on the pore size distribution of the final SiC powders (see Fig. 29). Based on the above tests, the SiC powders prepared by the sol-gel process all exhibit a good hydrothermal stability, and corrosion and oxidation resistance.

The X-ray diffraction patterns of the SiC powder (made from the Sol2 via sol-gel technique) after being subjected to the hydrothermal stability test at 350°C for 24 hrs is shown in Figure 23. The material after the hydrothermal test remains to be pure  $\beta$ -SiC similar to that before the test. In addition, the pore size distribution of the SiC powder before and after the hydrothermal treatment appears similar as shown in Figure 24. However, the pore volume increases substantially after the hydrothermal stability test, possibly due to the carbon-steam reaction which generates additional pore volume. Additional study is required in this area to obtain concrete evidence about the hydrothermal stability of the SiC powder prepared from the sol-gel technique.

#### 4.4.2. The SiC Membranes

As previously noted the SiC membranes are prepared by dip-coating of substrates made of mixtures of powders which are pressed into disks and then calcined at high temperatures. These substrates are highly porous with a bimodal pore size distribution with one sharp peak centered around 4 nm (corresponding to the finer particle size powder) together with a much broader macroporous peak centered around 150 nm corresponding to the larger size powder (see Fig. 30). The He/Ar separation factor for this substrate is close to unity and He/Ar permeance is  $\sim 7.2 \times 10^{-7} \text{ m}^3/(\text{m}^2 \cdot \text{Pa} \cdot \text{sec})$ . The effect on Ar permeance and the corresponding separation factor of coating a number of SiC layers is shown in Figs. 31 and 32. The Ar permeance changes during the first coatings but remains unchanged after that. There is no dependence of the permeance on the transmembrane pressure gradient, which is also a good indicator of the lack of any substantial convective flow contributions to the membrane transport. These observations are also validated by the behavior of the separation factor with the number of coatings (Fig. 32). After the third coating the measured separation factors are very close to the ideal Knudsen value of 3.16. AFM has also been used to study the surface morphology of the sol-gel coated samples. Figure 9 shows the AFM image of the SiC sol-gel membrane. There are no cracks and/or pinholes observed in the membrane layer, and the surface appears to be relatively smooth. Figure 32 shows the XRD pattern of the SiC membrane together with the XRD pattern of one of the powders prepared under similar conditions. The two XRD patterns are indistinguishable with the peaks corresponding primarily to  $\beta$ -SiC and with a very small quantity of  $\alpha$ -SiC phase also being present.

The SiC membranes were also subjected to the same hydrothermal test the various powders went through. The test, as previously, was carried out by exposing the membranes at 350 °C to a flowing mixture consisting of 50-mol% of water and 50-mol% of argon for a period of 30 h (the test was terminated after this period because there was no noticeable change in the membrane properties). During the test the argon permeation rate through the membrane was constantly monitored, and the results are shown in Fig. 33. The argon permeance remained constant throughout the whole period the membrane was exposed to steam. After the hydrothermal test the membrane separation characteristics were also studied by measuring the permeation rate of He and Ar. No noticeable changes were observed in the membrane transport characteristics, as can be seen in Figs. 31 and 32 which show the Ar permeance and the He/Ar separation factor as a function of transmembrane pressure gradient for the membrane before and after the hydrothermal test. Figure 34 shows an SEM picture of a cross section of the SiC membrane after the hydrothermal stability test. The sol-gel SiC thin film ( $\sim 4\text{-}5 \mu\text{m}$  thick) lies on the top of the macroporous SiC disk. It appears to be strongly adhering without any visible cracks or pinholes developing after the hydrothermal stability test.

To further investigate the ability of these materials to withstand the various corrosive environments, the various samples were analyzed by XPS. The XPS data are collected by a Perkin-Elmer /Physical Electronics Division model 5100 X-ray photoelectron spectrometer with a non-monochromatic Al K $\alpha$  1486.6 eV radiation source (15 kV, 300 W). Data acquisition and instrument control is performed using an RBD model 147 controller with Augerscan™ software. The samples, after being subjected to the various treatments, they are placed into the

analysis chamber and allowed to outgas until a vacuum of  $< 1 \times 10^{-7}$  torr had been restored (typical analysis pressure was in the range of  $1 - 8 \times 10^{-8}$  torr). Figure 35, for example, shows the XPS results of a powder SiC sample, which after being treated by HF for 5 h, air at 420°C for 3 h was subjected to a steam treatment. There is a strong peak at 100.4-101.0eV corresponding to SiC, which is indicative that the sample is silicon carbide (deconvolution of the spectra indicates the SiC content to be in excess of 94%). A small side shoulder at 103.0-103.3eV corresponds to a trace impurity of SiO<sub>2</sub>, which may be either a remnant of the original sol, or most likely due to the surface oxidation of the SiC as a result of the air oxidation and steam treatments. The XPS results seem to be consistent with the results of the XRD analysis.

## 4.5 Product Development and Process Simulation for WGS

### 4.5.1 Characterization of Hydrogen Selective Membrane prepared for WGS

In this section, we summarize the experimental results obtained from the characterization of the hydrogen selective membrane selected and its hydrothermal stability for the proposed WGS reaction. They are presented as follows:

- **Membrane Permeance and Selectivity**

Membrane hydrogen permeances ranging from 0.5 to  $>3 \text{ m}^3/\text{m}^2/\text{hr}/\text{bar}$  have been demonstrated (see Figures 37&38). Selectivities for H<sub>2</sub> to N<sub>2</sub><sup>4</sup> are 50 to  $>200$  even at temperatures in excess of 200°C as shown in these figures..

- **Hydrothermal Stability**

The hydrogen selective membrane has demonstrated excellent hydrothermal stability under the WGS condition we selected as shown in Figure 39. In addition, our hydrogen selective membrane has shown no aging effect during the 6-month storage test as shown in Figures 37&38.

### 4.5.2 Hydrogen Separation using Pilot Scale Hydrogen Selective Membrane

Figure 40 below shows the separation efficiency of one of M&P's full-scale hydrogen selective membranes generated from a pilot testing facility. The purity of hydrogen produced is plotted as a function of the percent of hydrogen recovered from a feed stream containing H<sub>2</sub>/CO at 50/50. High recovery of hydrogen is important and, as this figure shows, it is possible to recover 90% of the hydrogen in the feed gas at a product purity of ~90% H<sub>2</sub>. This stream represents the actual stream generated from our client's high temperature waste conversion process. In the WGS reaction, H<sub>2</sub> purity in excess of 99% is feasible as demonstrated in Figure 43 by coupling a similar stream generated from the coal gasifier with a water-gas-shift reaction.

### 4.5.3 Comparison of Membrane vs Conventional Reactor for WGS – Mathematical Simulation

Presently, WGS is implemented in a two-stage operation. A high temperature shift reactor (HTS) is operated at ~450°C to take advantage of the high reaction rate and deliver about 97% conversion [32]. Also, excess steam (6 to 10 times stoichiometric requirement) is used to promote conversion and inhibit catalyst coking. Then, a low temperature shift (LTS) at ~200 to 250°C is used to further increase the CO conversion to ~99.2 to 99.6% [32]. Again, excess steam is used to promote equilibrium conversion but coke formation potential is negligible. However, the reaction rate is too low at this low temperature due to the high hydrogen concentration. Yet, if the reaction rate can be enhanced via in-situ removal of hydrogen, the LTS operation is very attractive since:

- ❑ Single stage conversion of CO from 0 to  $>99.9\%$  can be achieved at low temperature
- ❑ Excess steam can be minimized since coke formation potential is negligible.
- ❑ The low reaction rate in LTS can be compensated for via in-situ removal of hydrogen.

---

<sup>4</sup> Nitrogen is used here to represent gas components rejected by this hydrogen selective membrane, including CO<sub>2</sub> and CO. Water, as H<sub>2</sub>, is permeable through the membrane.

The simulation presented in Figure 41 shows that conversion vs reactor length for a side-by-side conversion (i.e., same superficial space velocity and catalyst loading) of the proposed membrane reactor vs the low temperature shift (LTS) reactor. Both are operated at 250°C, a maximum operating temperature of existing LTS reactor, and H<sub>2</sub>O/CO ratio of 6, the low end of the conventional WGS reaction. Evidently, the packed-bed reactor is very inefficient under LTS conditions due to the low reaction rate in the presence of substantial product hydrogen. Hence, the 2<sup>nd</sup> stage is only used to improve the conversion of CO typically from 92 to 99%. On the other hand, the MR can selectively permeate hydrogen throughout the entire bed length; thus, the conversion of CO in the membrane reactor exceeds the packed-bed reactor, i.e., from 0 to 99.9%. In summary, the WGS-MR operated at the LTS range is technically feasible based upon the simulation result here using the rate parameters and operating condition presently practiced for the LTS reactor.

#### 4.5.4 Projected Benefit of Using MR for WGS

The essence of this proposed WGS-MR is its ability to deliver high CO conversion under the mild LTS operating conditions. Thus, the WGS reaction for coal-based power generation can be streamlined to a single stage using one type of catalyst and operated at one temperature as opposed to the conventional use of two different catalysts at two reaction temperatures. In addition to the capital cost savings with this one stage operation at the lower temperature, we have identified additional benefits below:

- ❑ Cost Savings via Reduced Steam/CO Ratio. Steam in excess of stoichiometry is not required since coke formation potential is negligible and isothermal operation is simplified using the MR configured as a shell-and-tube heat exchanger. Our simulation below shows the effect of the steam/CO ratio at 6, 3 and 1.5 for the membrane reactor and 6 for the packed bed (see Figure 42). Evidently, the conversion difference between 1.5 and 6 is modest. In fact, the low ratio favors a high degree of hydrogen recovery as discussed next.
- ❑ Hydrogen Recovery with Minimum Parasitic Energy Consumption. In our simulation presented in Figure 43 hydrogen is recovered in the MR by sweeping the permeate with steam (at ca. 25% of the feed). Thus the majority of the H<sub>2</sub> can be recovered using a small amount of near ambient steam. Water can then be knocked out of the hydrogen (and recycled if necessary). Thus, our simulation shows that using WGS-MR, a high degree of hydrogen recovery can be accomplished with minimal parasitic energy consumption.
- ❑ Trace CO Contamination of the Recovered Hydrogen. CO content in the hydrogen product is critical for the down stream power generation via the PEM type fuel cell. Our simulation in Figure 44 indicates that CO as low as ~200 ppm can be achieved with the proposed WGS-MR. This trace level of CO can be post treated with a methanizer or partial oxidizer economically and effectively to reduce it to <10 ppm to meet the present PEM fuel cell feedstock specification. For comparison, the conventional WGS delivers ~0.3mole %CO at the exit stream of the LTS reactor [32]. Thus, the cost of post-treatment to meet the fuel cell specification is much reduced in the proposed MR.
- ❑ Streamline of Pre-treatment Requirement. No simulation can quantify this benefit although we believe that the potential cost savings are significant.

## 5. CONCLUSIONS

Major activities carried out during of this project include membrane preparation, gas separation characterization, hydrothermal stability testing, and WGS process simulation. Key conclusions from this study are drawn as follows:

### Preparation of SiC Substrates

Silicon carbide (SiC) macroporous and meso-/micro-porous membranes were successfully prepared as potential substrates for the SiC-based H<sub>2</sub> selective membrane. Composite SiC based membranes with pore sizes of 40Å to >0.1µm were prepared with consistent quality. The macroporous SiC substrate was prepared by pressing commercial SiC powder into disk with aluminum, boron, and/or carbon as a binder; then the disk was calcined at >2,000°C. The resultant membranes were characterized by the pore size distribution analysis, gas permeance measurement, XRD and SEM. The meso-/micro-porous SiC membrane was prepared by deposition of (i) polycarbosilane (as a precursor), or (ii) SiC precursor sol on the SiC macroporous substrate, then calcined at

~1,400°C. The conversion of polycarbosilane and the sol to SiC at this temperature was verified with XRD analysis. In addition, this mesoporous membrane was characterized by the helium and nitrogen gas permeance and BET surface area as an indicator of pore size distribution.

#### Preparation of Hydrogen Selective SiC Membranes via CVD/I

Hydrogen selective nanoporous SiC-based membranes were successfully prepared using a chemical vapor deposition/infiltration (CVD/I) technique developed by M&P. CVD/I conditions were investigated under the assistance of on-line helium and nitrogen measurement. Deposition at 750°C with subsequent calcination at 1,000°C was selected for further membrane preparation and gas permeation study. A total of 12 membranes were successfully developed under this task for gas permeance and hydrothermal stability tests. In addition, unsupported SiC film, i.e., SiC powder, was generated under a similar condition for surface analysis. This powder after calcination at 1,000, 1,200 and 1,400°C was examined using XRD to confirm the formation of SiC and its crystal formation.

#### Preparation of Hydrogen selective SiC Membranes via Pyrolysis of Pre-Ceramic Polymers

SiC hydrogen selective membrane via pyrolysis of pre-ceramic polymers was explored as an alternative to CVD/I. The membranes were prepared with multiple coating/pyrolysis (3 times) of allyl-hydridopolycarbosilane (AHPCS) in order to reach a desirable separation efficiency, i.e., >20 for He/N<sub>2</sub> at 200°C. This pre-ceramic polymer generates a porous structure of ~5Å in pore size under the proposed pyrolysis temperature (i.e., 600°C). Whether the selection of 600°C is sufficient to deliver a membrane material with a satisfactory hydrothermal stability remains to be evaluated.

#### Mechanical Stability Tests of SiC Membranes

SiC membrane prepared via CVD on the commercial Al<sub>2</sub>O<sub>3</sub> macroporous substrate (available from M&P) was subjected a heating and cooling study to determine its impact on the microporous layer structure and its physical attachment. Membranes prepared at 750°C and calcined at 1,000°C went through the heating cycling twice in this study. Gas permeation rate remains similar for the sample through the heating/cooling cycles. The mechanical stability of the SiC/Al<sub>2</sub>O<sub>3</sub> composite membrane is thus confirmed at 25 to 1,000°C in inert atmosphere. Additional tests in the presence of the high pressure steam is required to determine the thermal mismatch between SiC and SiC/Al<sub>2</sub>O<sub>3</sub> under the proposed WGS environment. Then the selection between SiC/SiC and SiC/Al<sub>2</sub>O<sub>3</sub> will be made for membrane manufacturing in the future.

#### Thermal and Hydrothermal Stability Test

The hydrogen selective nanoporous SiC membranes prepared under this project displayed excellent thermal and hydrothermal stability. No loss in permeance or selectivity was observed with a SiC hydrogen selective membrane in a roughly 100 hour hydrothermal test conducted at 750°C and 50% steam (at atmospheric pressure). In addition, thermal stability was conducted very briefly. Since the membrane was calcined at 1000°C, its thermal stability at 750°C is expected to be excellent.

#### Gas Separation Study

Gas separation characteristics of the hydrogen selective membrane prepared in this study was determined its single gas permeation of hydrogen helium, nitrogen, CO<sub>2</sub> and CH<sub>4</sub>. Depending upon the deposition and calcination conditions, the nanoporous membranes produced displayed a high helium permeance of 0.65 to 13.9 m<sup>3</sup>/m<sup>2</sup>/hr/bar and high selectivities for He over N<sub>2</sub>, CO<sub>2</sub>, and CH<sub>4</sub> of 4 to 85.

#### WGS process simulation

Our in-house simulation study indicates nearly complete conversion of CO and recovery of hydrogen from the coal gasifier off-gas via the one-stage water-gas-shift (WGS) reaction operated in the LTS range using an MR. Specific benefits include:

- Complete conversion of CO in a single -stage WGS-MR under mild conditions, i.e., existing low-temperature-shift (LTS) reaction temperature, 200 to 250°C, and catalyst with a stoichiometric steam/CO ratio.
- Concentration of CO<sub>2</sub> in the reject side of MR for CO<sub>2</sub> capture with *minimum or no* parasitic energy consumptions.
- Reducing gas clean-up burden via pre-treatment at a manageable temperature, e.g., 250°C vs >450°C of existing hot gas clean-up.

In summary our study has demonstrated (i) the technical feasibility of preparing SiC- based H<sub>2</sub> selective membrane via the proposed approaches and (ii) their improved hydrothermal stability. In addition, the potential benefits of using this membrane as a membrane reactor for WGS reaction have been identified in this study.

Table 1. Helium and Nitrogen Permeances of Mesoporous SiC Membranes Prepared via Calcination of Polycarbosilane

Gas	Pressure Gradient (psi)	Permeance (k) <sup>+</sup> (cm <sup>3</sup> /cm <sup>2</sup> .psi.min)	Separation Factor* (He/N <sub>2</sub> )
Helium (He)	40	0.0476	2.90
	30	0.0482	2.80
	20	0.0486	3.00
	10	0.0497	3.25
Nitrogen (N <sub>2</sub> )	40	0.0164	-
	30	0.0172	-
	20	0.0162	-
	10	0.0153	-

\* Ideal separator factor is 2.65

+ 25°C.

**Table 2** Permeance of SiC Membranes after CVD/I at 750°C and After Calcination at 1000°C

Sample ID	Membrane precursor (pore size)	Before CVD/I (starting membrane)			After CVD/I			After Calcination			After cooling to 25C		
		Permeance(M3/M2/hr/bar) @750C			Permeance(M3/M2/hr/bar) @750C			Permeance(M3/M2/hr/bar) @1000C			Permeance(M3/M2/hr/bar) @25C		
		He	N2	Selectivity	He	N2	Selectivity	He	N2	Selectivity	He	N2	Selectivity
TPS-003	100A	36.80	19.80	2.37	7.03	0.08	92.50	0.65	0.05	13.95	0.32	0.12	2.71
TPS-010	100A	47.30	18.80	2.52	0.95	0.04	26.85	1.55	0.03	59.16	12.40	5.90	2.10 crack
TPS-017	100A	59.10	22.20	2.65	1.97	0.12	16.55	(not heated to 1000C)			0.36	0.77	0.46
TPS-021	100A	52.80	19.40	2.72	3.63	0.02	197.28	7.41	1.69	4.38	no data		
TPS-006B	100A	61.80	24.80	2.49	0.89	0.01	72.62	0.85	0.01	84.60	0.09	0.05	1.91
TPS-007B	100A	61.10	23.50	2.60	9.26	0.02	557.83	13.90	1.07	12.99	no data crack		
TPS-013B	100A	13.80	5.19	2.66	1.28	0.08	16.26	0.74	0.05	15.79	no data		
TPS-017B	100A	68.8	28.6	2.59*	11.88	0.201	59.10	2.58	very low	-			
TPS-019B	100A	73.5	28.6	2.57*	4.78	0.0334	143.11	no data	no data	-			
TPS-020B	100A	74.6	35.9	2.08*	4.94	0.0651	58.05	1.47	0.0217	67.74			
TPS-021B	100A	61.7	25.5	2.42*	7.48	1.29	5.80	?	1.22	-			
TPS-022B	100A	63.1	24.6	2.57*	8.11	0.0574	141.29	no data	no data	-			

\* 700°C

**Notes:**

- Helium was used as a surrogate gas for hydrogen. Nitrogen was used to represent CO<sub>2</sub>, CH<sub>4</sub>, etc.
- The wide range of permeance and selectivity reflects our evaluation of several key deposition parameters as part of the feasibility study. For a perspective on reproducibility, see Sec. 3.2 C
- As a general trend (5 out of 7 samples), performance after conversion to SiC (after calcination) follows that after CVD/I. Thus, on-line monitoring of performance during CVD/I was used as a control parameter for CVD/I in this study.

**Table 3. Permeance vs. Temperature for SiC H<sub>2</sub>-Selective Membranes Prepared With CVD/I Technique at 700°C**

	<u>300°C</u>	<u>400°C</u>	<u>500°C</u>	<u>600°C</u>	<u>1,000°C</u>
<b>TPS-17B</b>					
He permeance (m <sup>3</sup> /m <sup>2</sup> /hr-bar)	1.11	1.39		3.32	
N <sub>2</sub> permeance (m <sup>3</sup> /m <sup>2</sup> /hr-bar)		0.03		0.04	
Separation factor		51.48		85.13	
<b>TPS-19B</b>					
He permeance (m <sup>3</sup> /m <sup>2</sup> /hr-bar)		0.05		0.65	
N <sub>2</sub> permeance (m <sup>3</sup> /m <sup>2</sup> /hr-bar)		0.21		0.04	
Separation factor		0.26		16.67	
<b>TPS-20B</b>					
He permeance (m <sup>3</sup> /m <sup>2</sup> /hr-bar)		0.19		0.42	1.47
N <sub>2</sub> permeance (m <sup>3</sup> /m <sup>2</sup> /hr-bar)		0.07		0.06	0.02
Separation factor		2.81		6.55	67.74
<b>TPS-21B</b>					
He permeance (m <sup>3</sup> /m <sup>2</sup> /hr-bar)		6.69		5.20	
N <sub>2</sub> permeance (m <sup>3</sup> /m <sup>2</sup> /hr-bar)		2.14		1.94	
Separation factor		3.13		2.68	
<b>TPS-22B</b>					
He permeance (m <sup>3</sup> /m <sup>2</sup> /hr-bar)		0.36		0.50	
N <sub>2</sub> permeance (m <sup>3</sup> /m <sup>2</sup> /hr-bar)		0.11		0.07	
Separation factor		3.14		7.26	

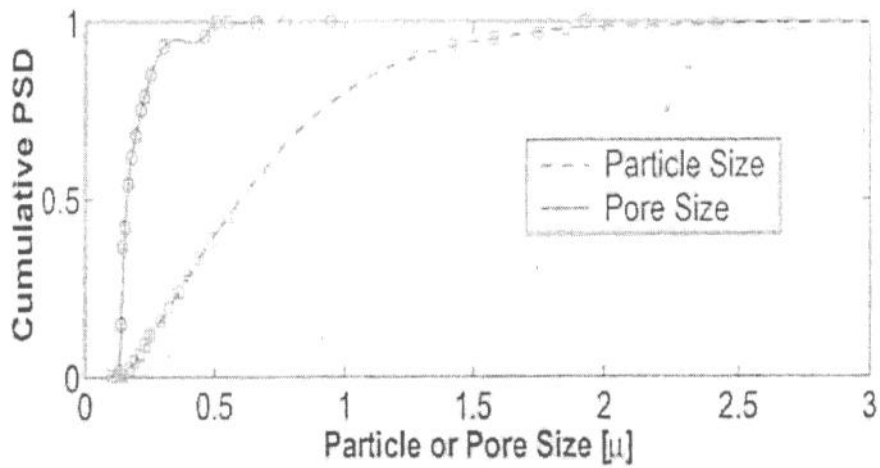


Figure 1. The cumulative particle and pore sizes distribution of substrate made from 1  $\mu$  (P1) average particle size powder.

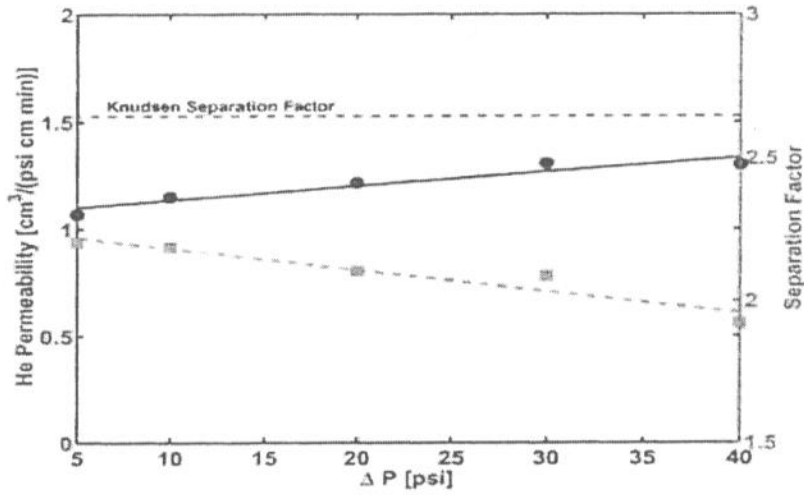


Figure 2. The permeability and separation factor of P1 substrate

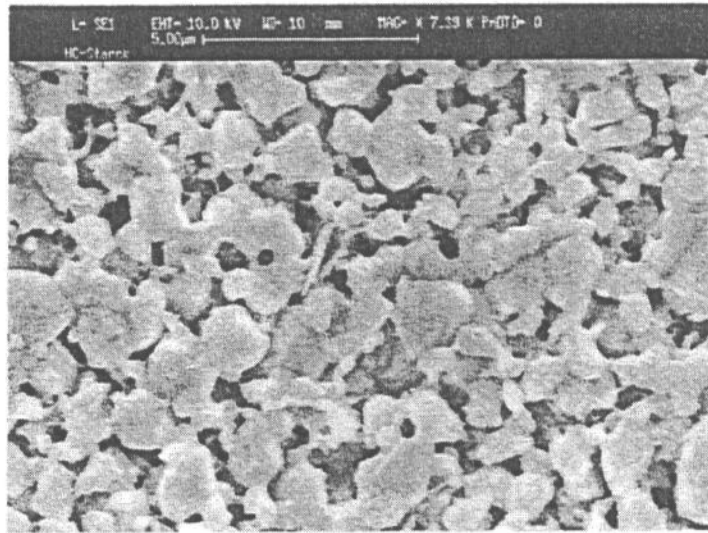


Figure 3. SEM photomicrograph of top surface of SiC macroporous substrate (P1)

*Horvath-Kawazoe Differential Pore Volume Plot  
Slit Pore Geometry (original HK)*

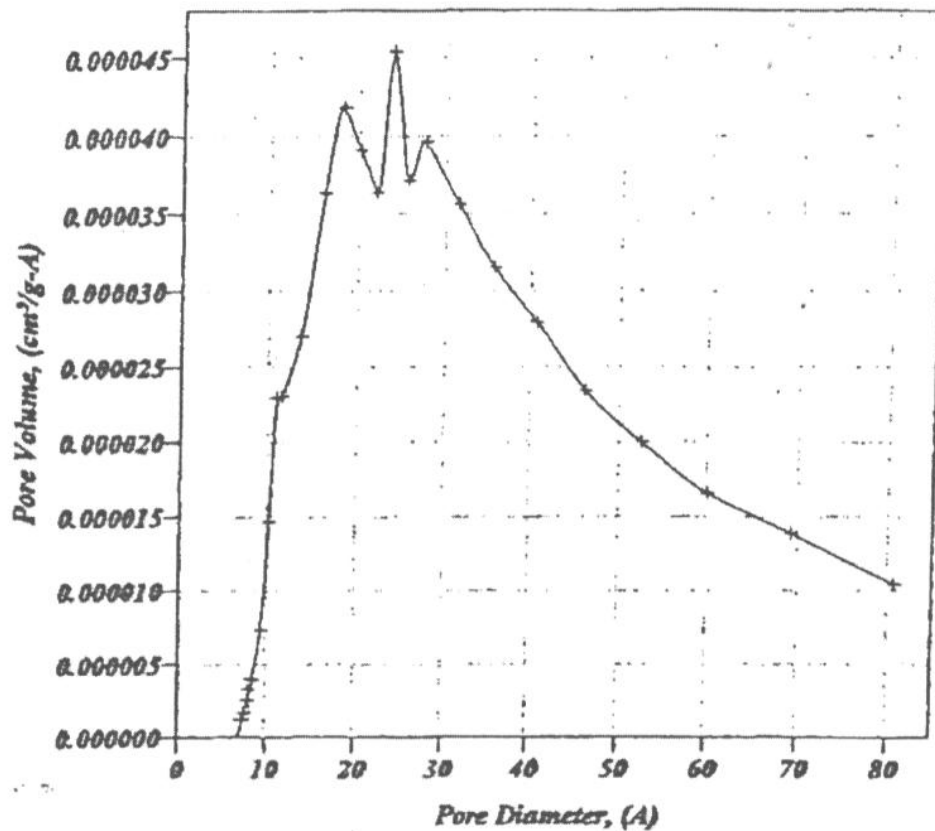


Figure 4. Pore size distribution (based on BET measurement) of SiC film prepared from calcination of polycarbosilane.

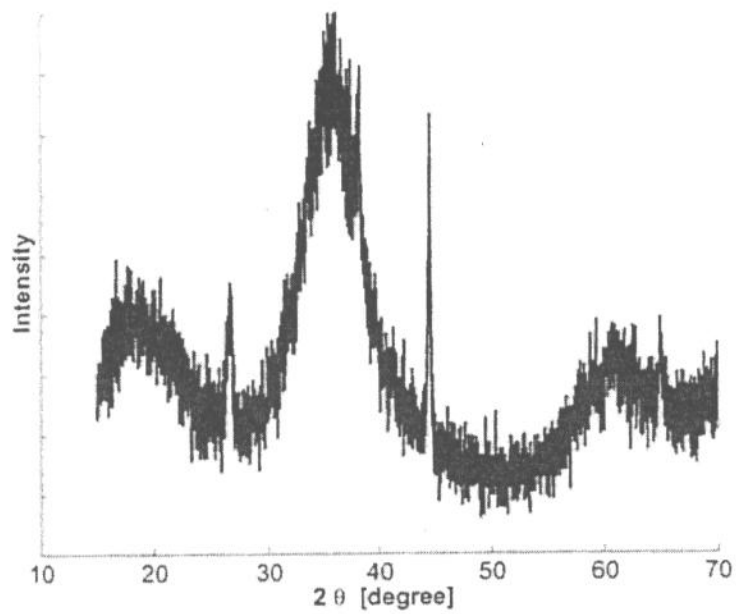


Figure 5. XRD pattern of SiC substrate prepared from calcination of polycarbosilane.

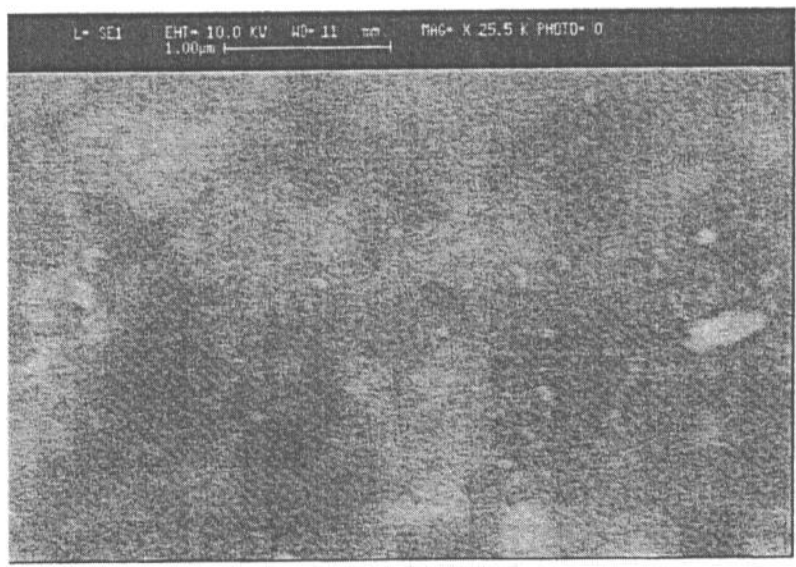
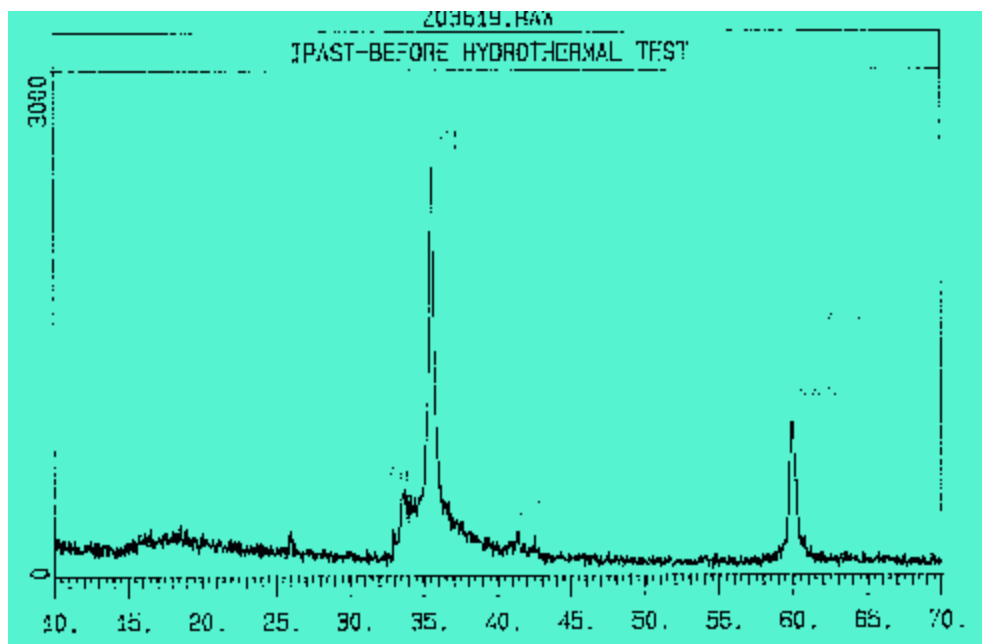
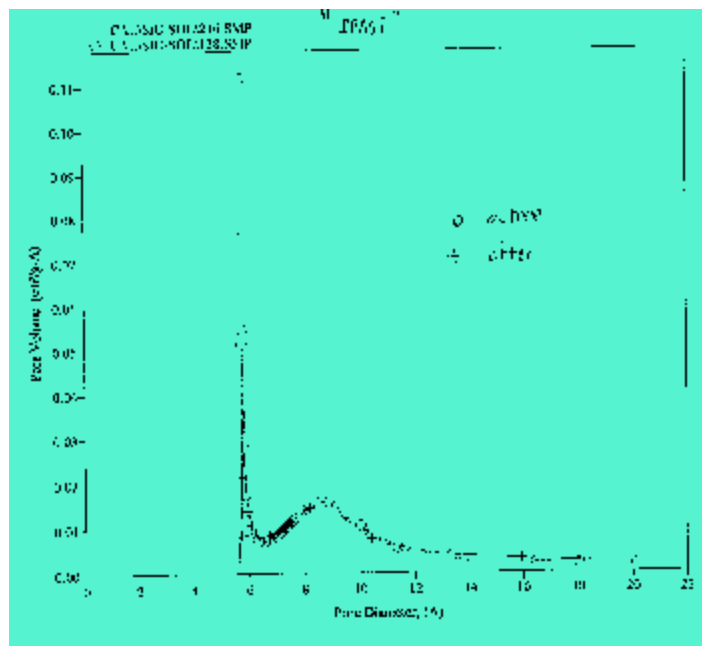


Figure 6. SEM photomicrograph (of top surface) of SiC microporous substrate prepared from calcination of polycarbosilane



**Figure 7. XRD pattern (b-SiC) of unsupported SiC thin film prepared with sol-gel technique.**



**Figure 8. Pore size distribution (based upon N<sub>2</sub> adsorption) SiC thin film prepared via sol-gel technique. Majority of pores range from 6 to 12Å**

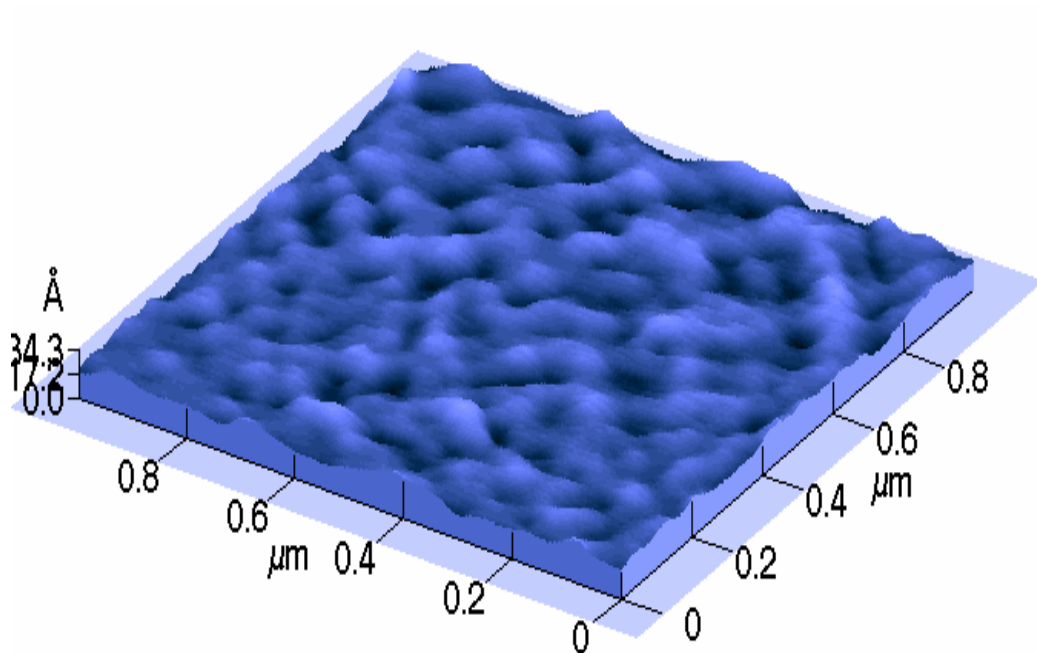


**Figure 9. Surface Topograph of Microporous SiC Membrane Prepared via Sol-gel Technique**

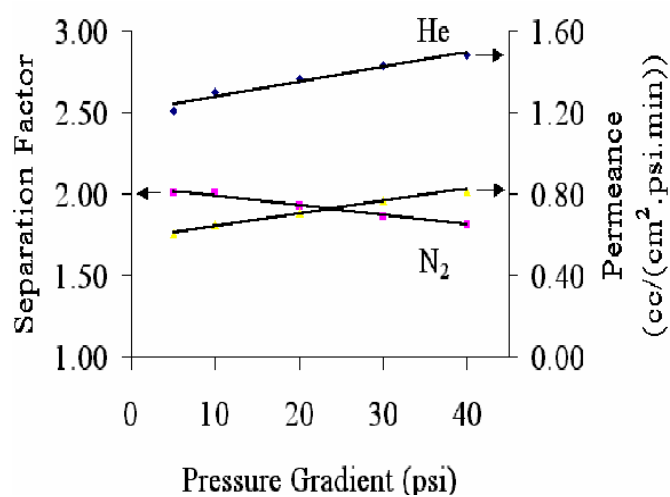


**Figure 10.** Gas permeance (single component) and separation factor vs. transmembrane pressure drop of microporous SiC membrane supported on SiC macroporous substrate. Calculated separation factor is close to the ideal separation factor based upon Knudsen diffusion, indicating a high quality nearly defect-free membrane.

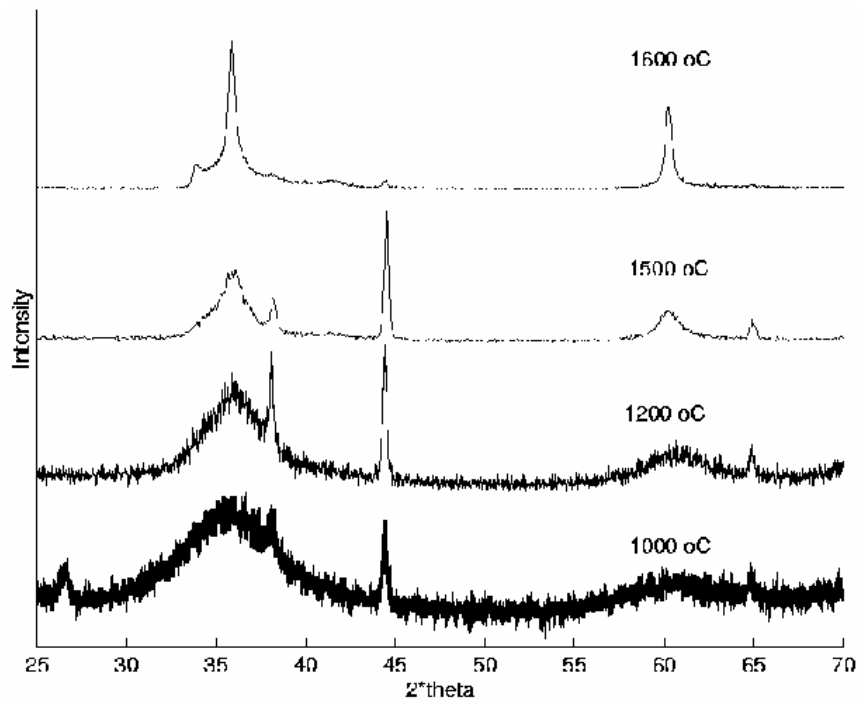
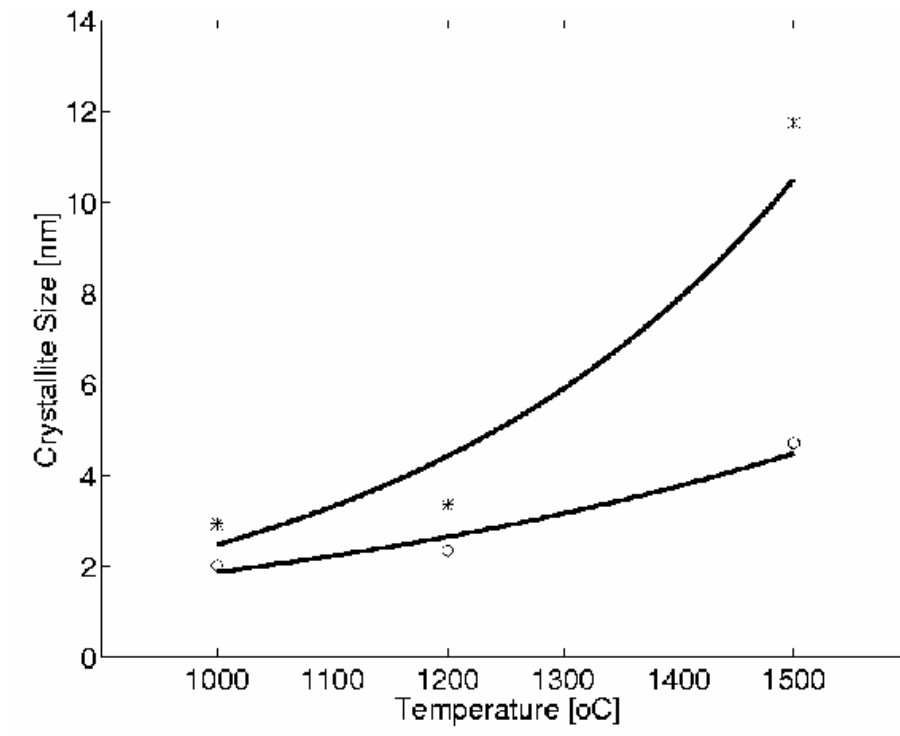


Figure 11. XRD pattern of SiC powder prepared from pre-ceramic polymer (AHPCS) calcined at 1,000 to 1,600 °C.



○ after 2<sup>nd</sup> pyrolysis

\* after 3<sup>rd</sup> pyrolysis

**Figure 12.** Calculated crystal size of the SiC powder prepared from pre-ceramic polymer (AHPCS) calcined at 1,000 to 1,500°C

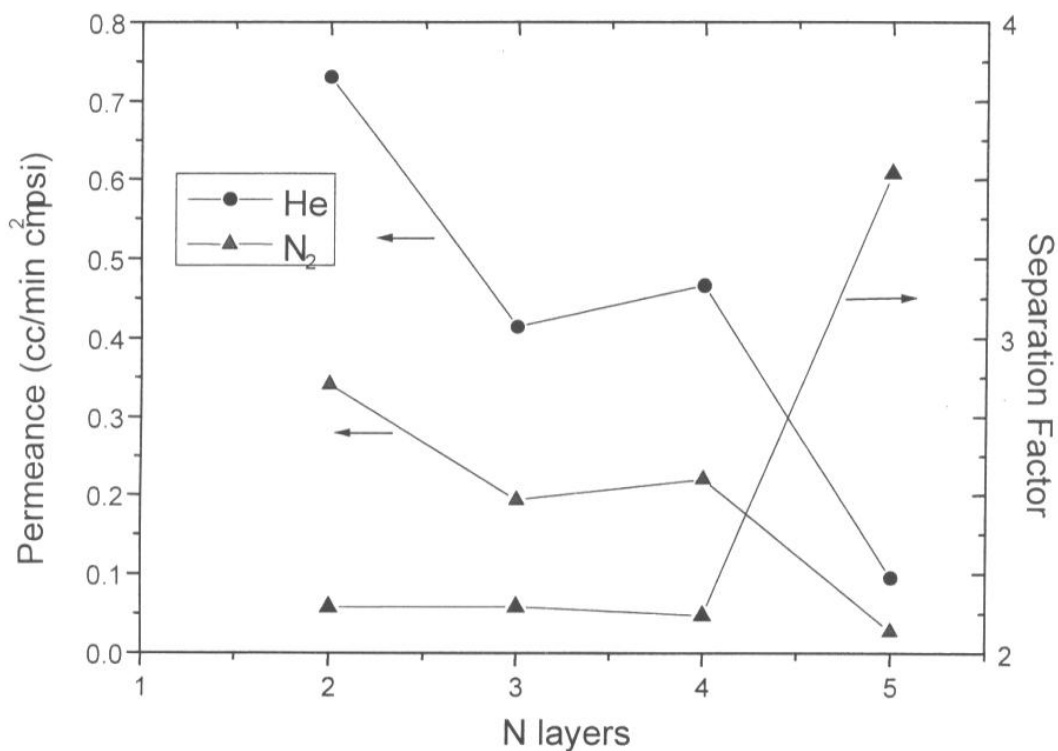


**Figure 13. Effect of the number of coatings on the permeance and separation factor (at room temperature) of SiC H<sub>2</sub> selective membranes prepared from pre-ceramic polymer (AHPCS) coated on SiC macroporous substrate.**

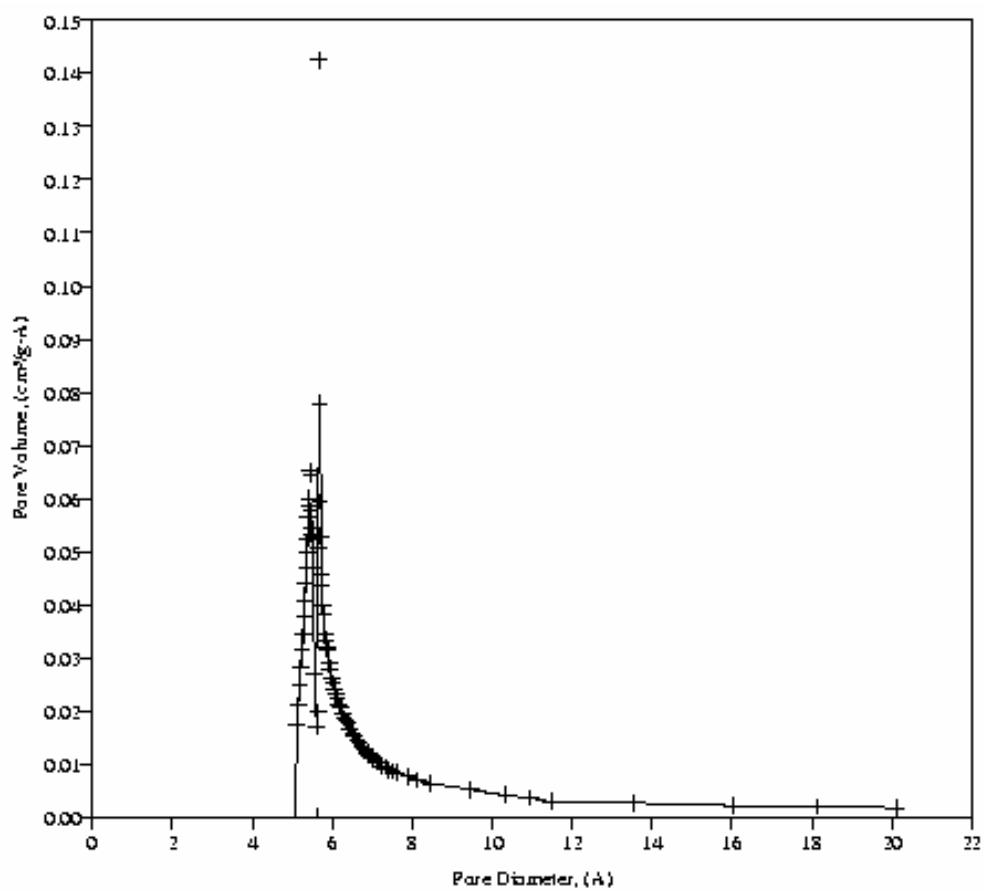
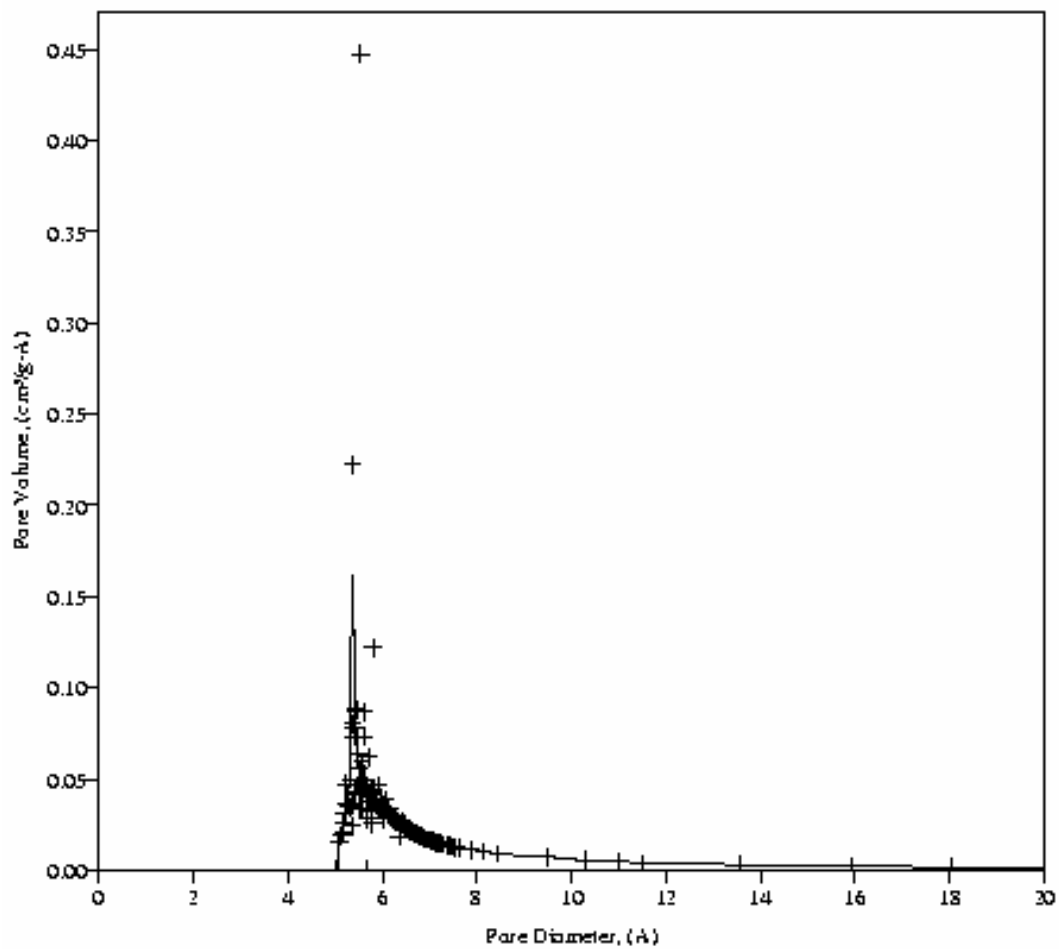
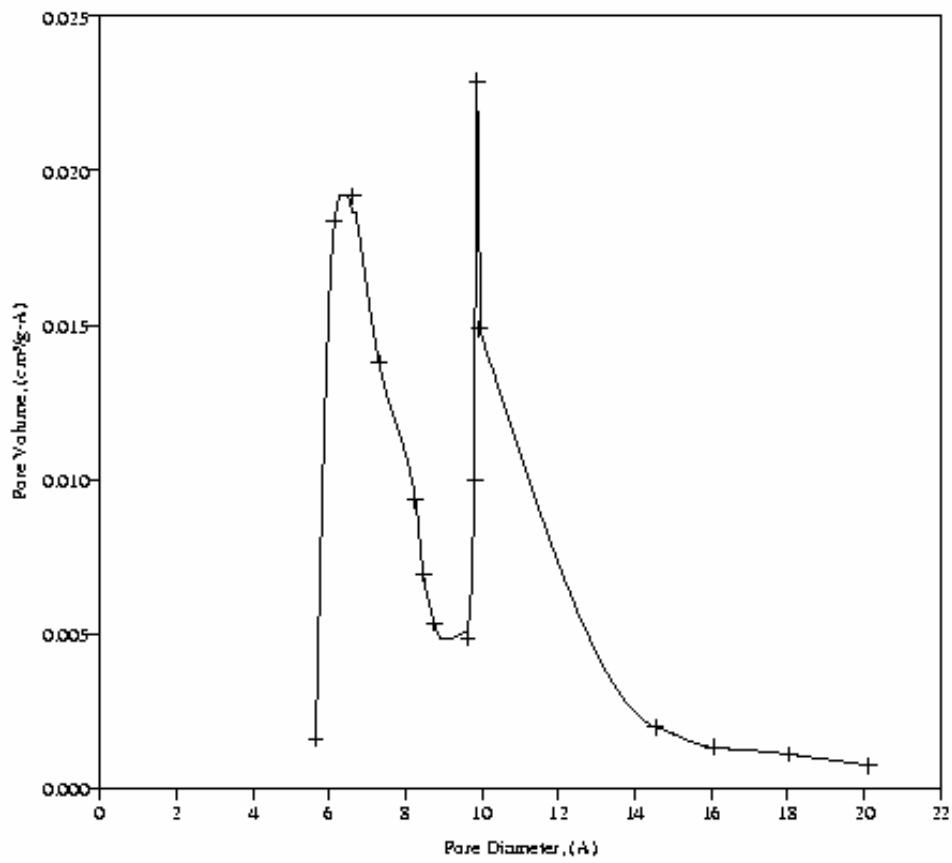
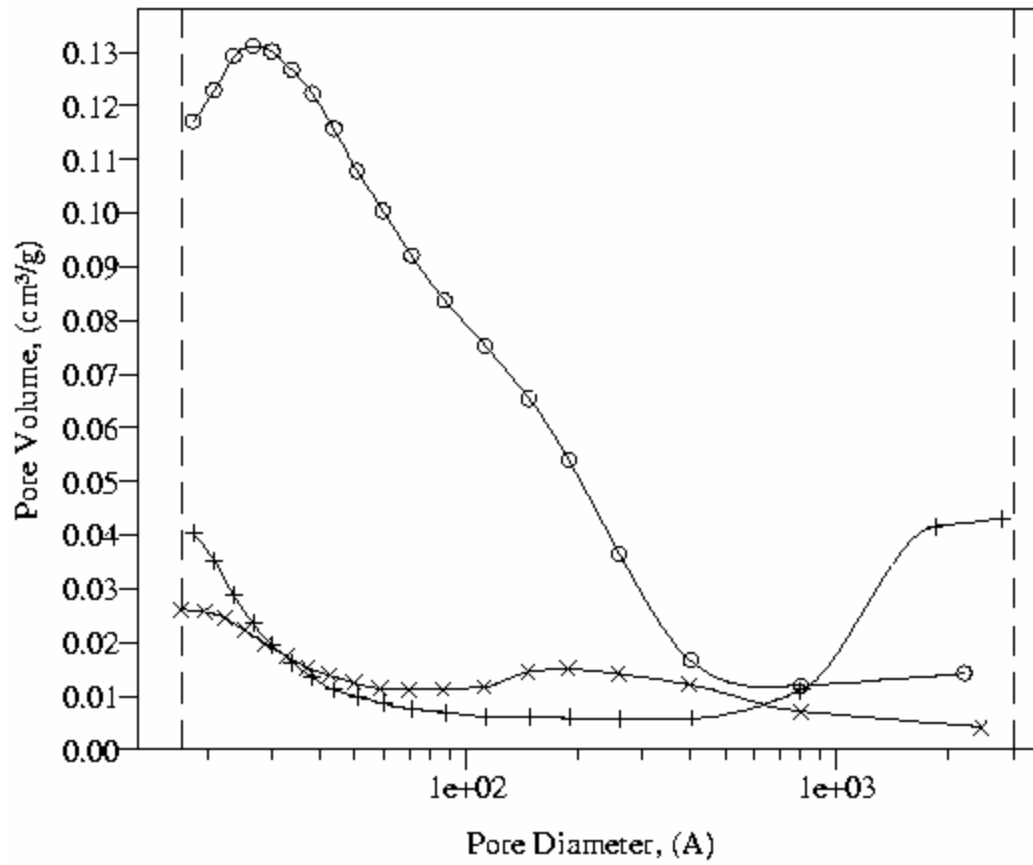


Figure 14. Pore size distribution (microporous range) of SiC powder prepared via pyrolysis (1<sup>s</sup>, 2<sup>nd</sup> and 3<sup>rd</sup>) of pre-ceramic powder





+ First Pyrolysis  
o Second Pyrolysis  
X Third Pyrolysis

**Figure 15. Pore size distribution (meso- and macro-porous range) of SiC powder prepared from pyrolysis of pre-ceramic polymer (AHPCS).**

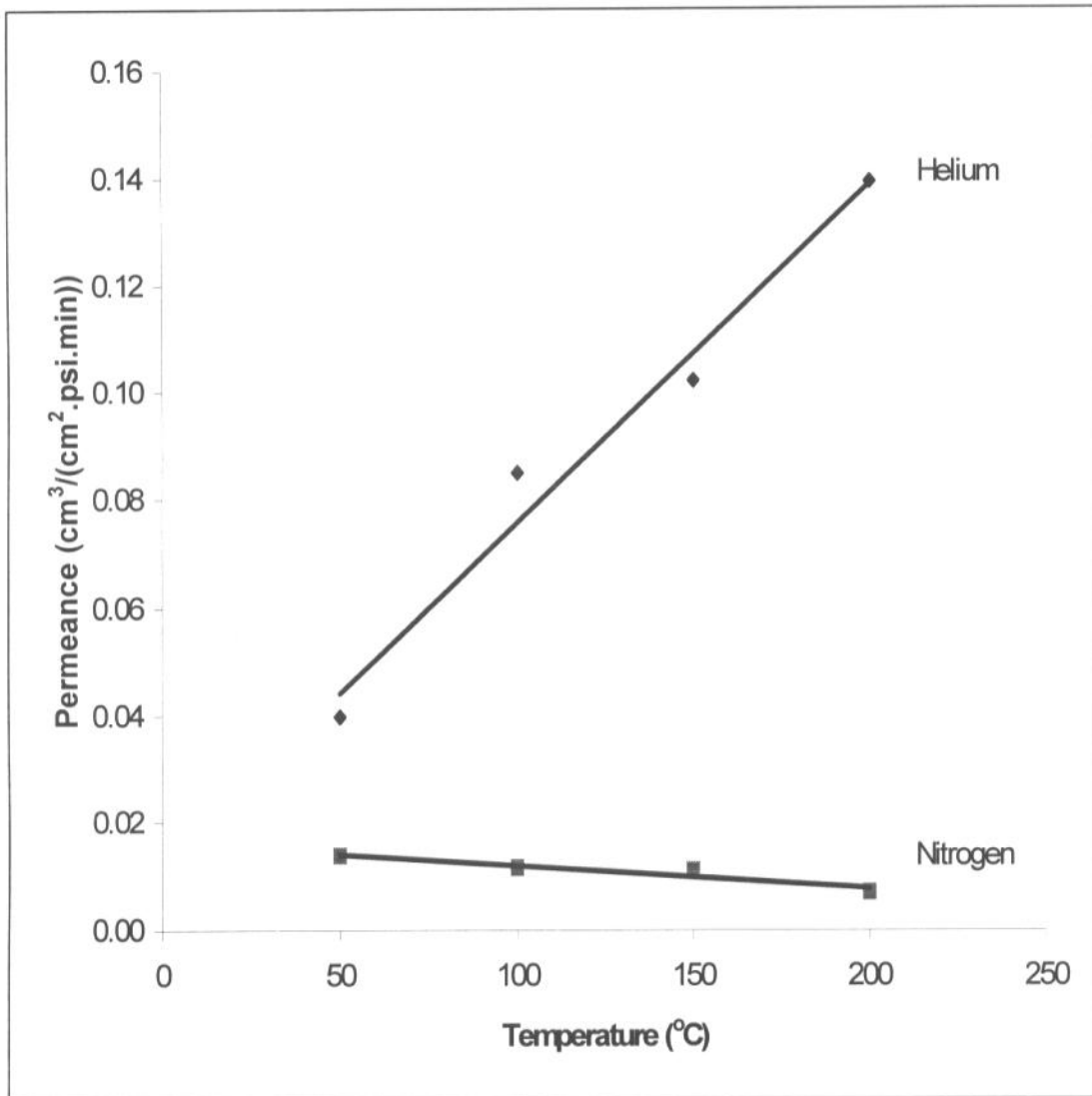
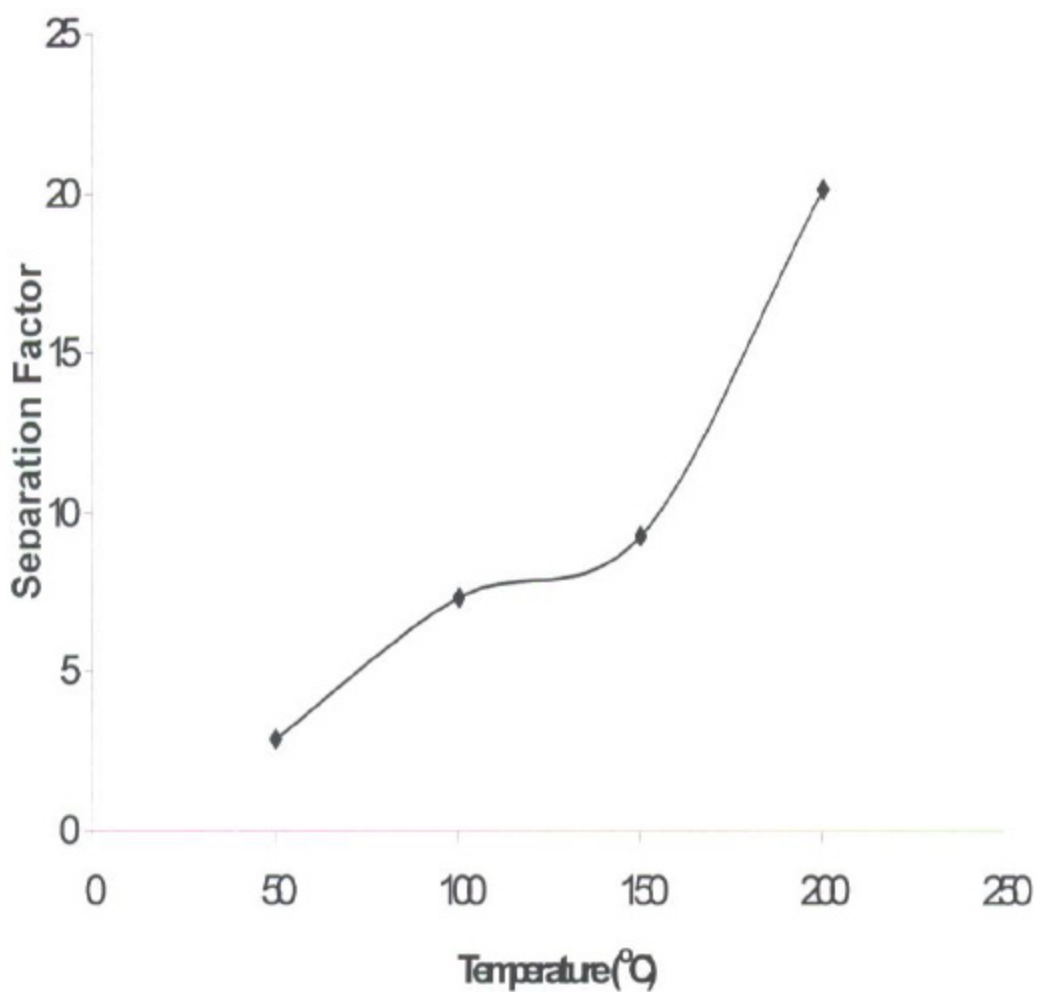
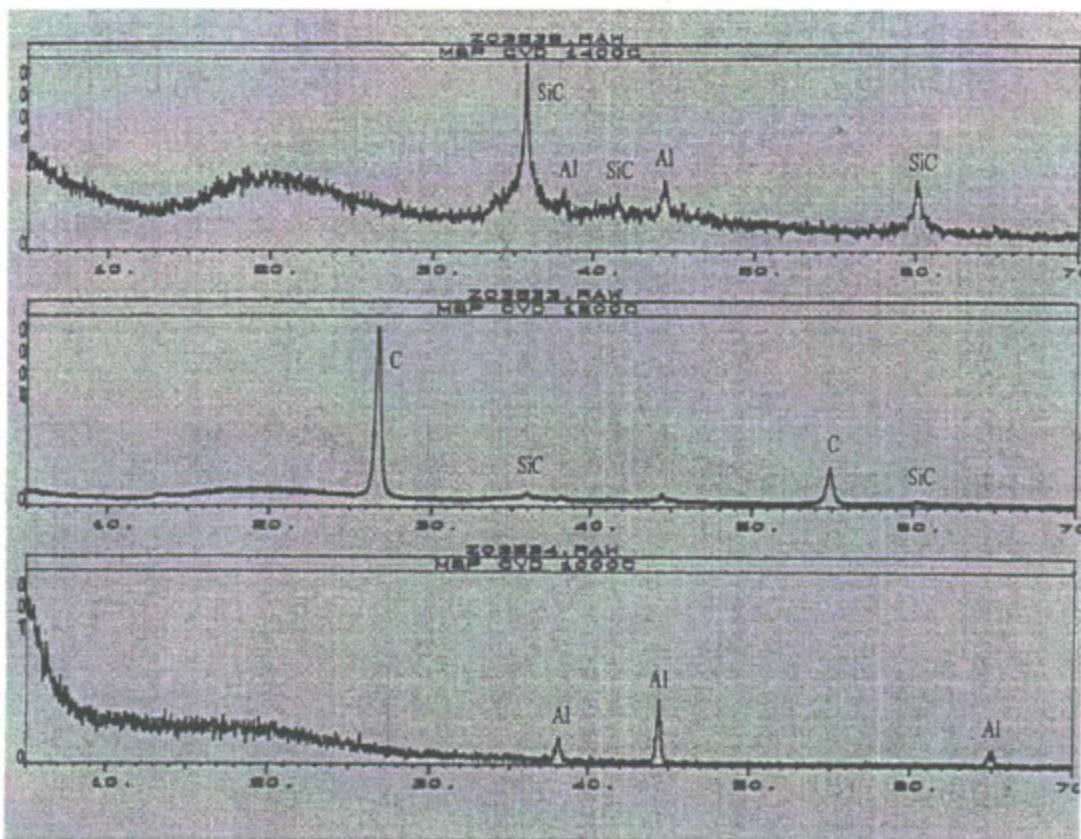


Figure 16. Permeance of N<sub>2</sub> and He as a function of temperature prepared from SiC pre-ceramic polymer (AHPCS coated) on SiC macroporous substrate.



**Figure 17. Separation factor (He/N<sub>2</sub>) vs. temperature of SiC H<sub>2</sub> selective membrane prepared with a pre-ceramic polymer (AHPCS) coated on SiC porous substrate. Permeance vs. temperature of this membrane is shown in Figure 16.**



**Figure 18.** XRD analyses of unsupported SiC films prepared via CVD/I at 750°C and calcined at 1,000 (bottom), 1,200 (middle), and 1,400°C (top). Degree of SiC crystallinity increases with the calcination temperature from 1,000 to 1,400°C. Excess carbon residue was observed at 1,200°C and is assumed to exist at 1,000°C but in the amorphous state. The aluminum present is likely from contamination of the samples.

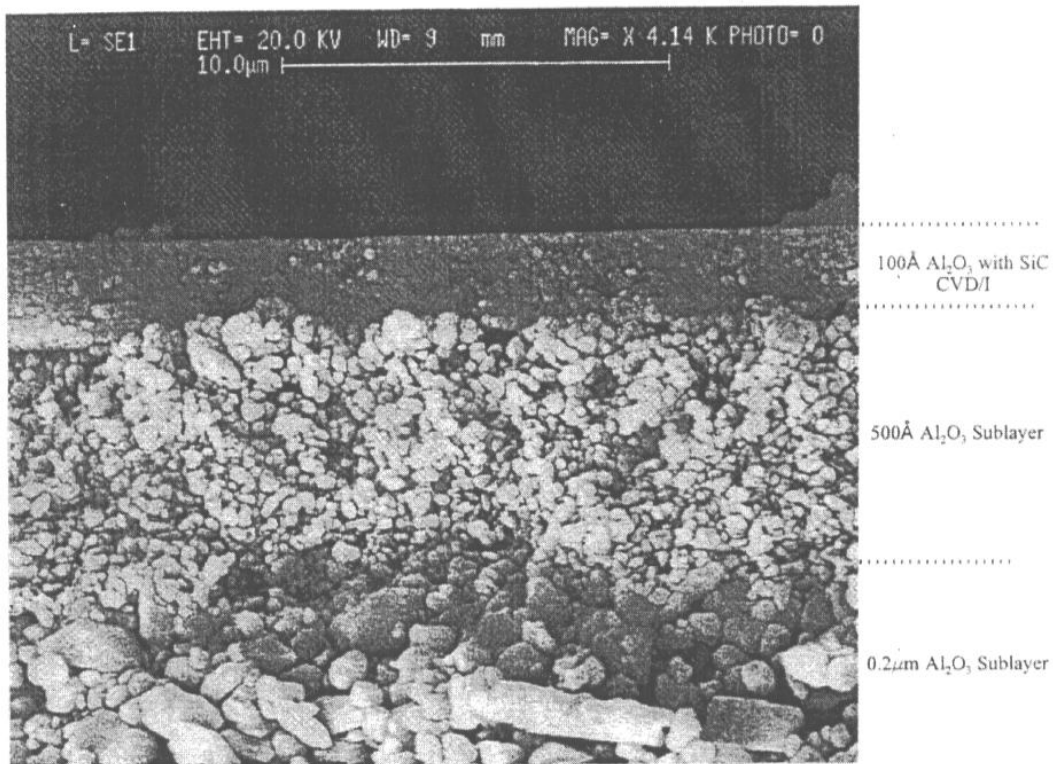


Figure 19a. SEM Photomicrograph of M&P's alumina microporous substrate (ca. 100Å) with SiC thin film deposition via CVD/I.

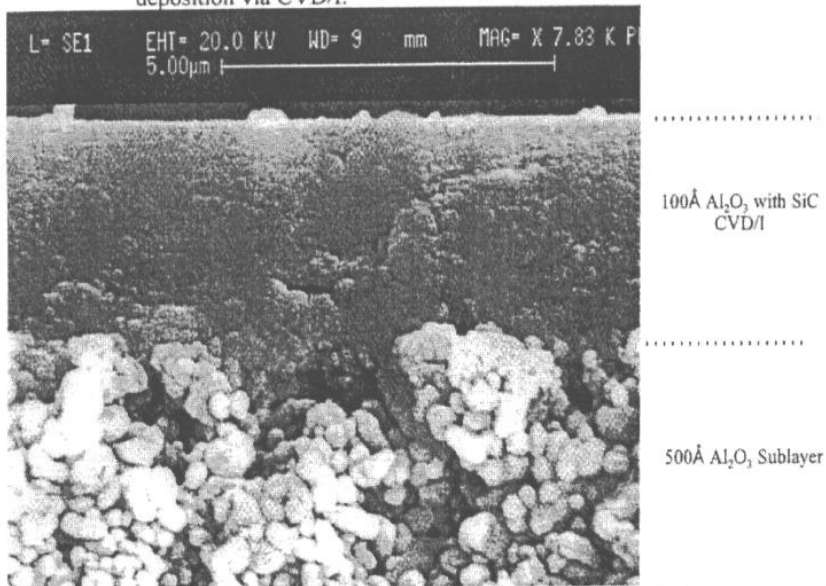


Figure 19b. Higher magnification showing that an extremely thin SiC film was deposited because no visible difference can be seen between the SiC at the top surface and the underlying alumina substrate

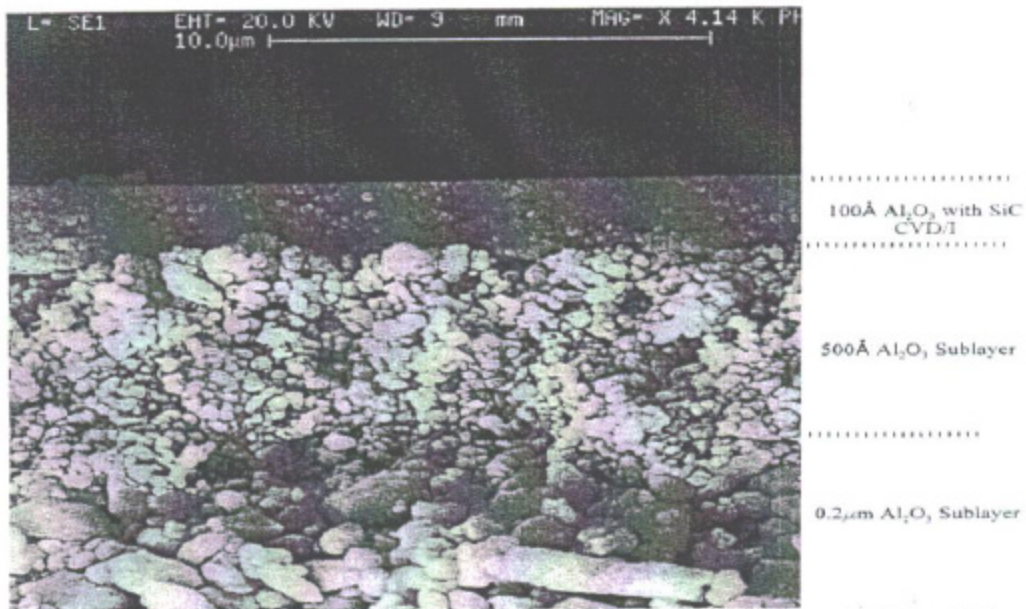
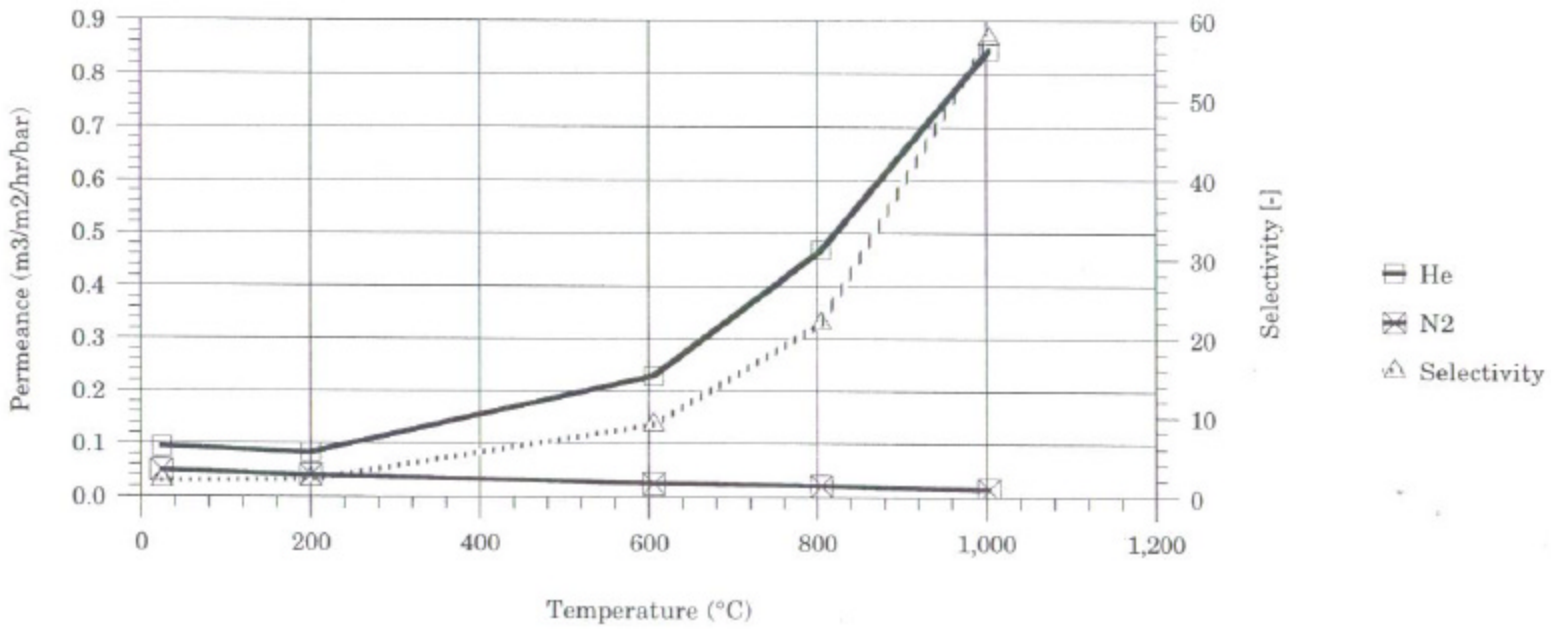


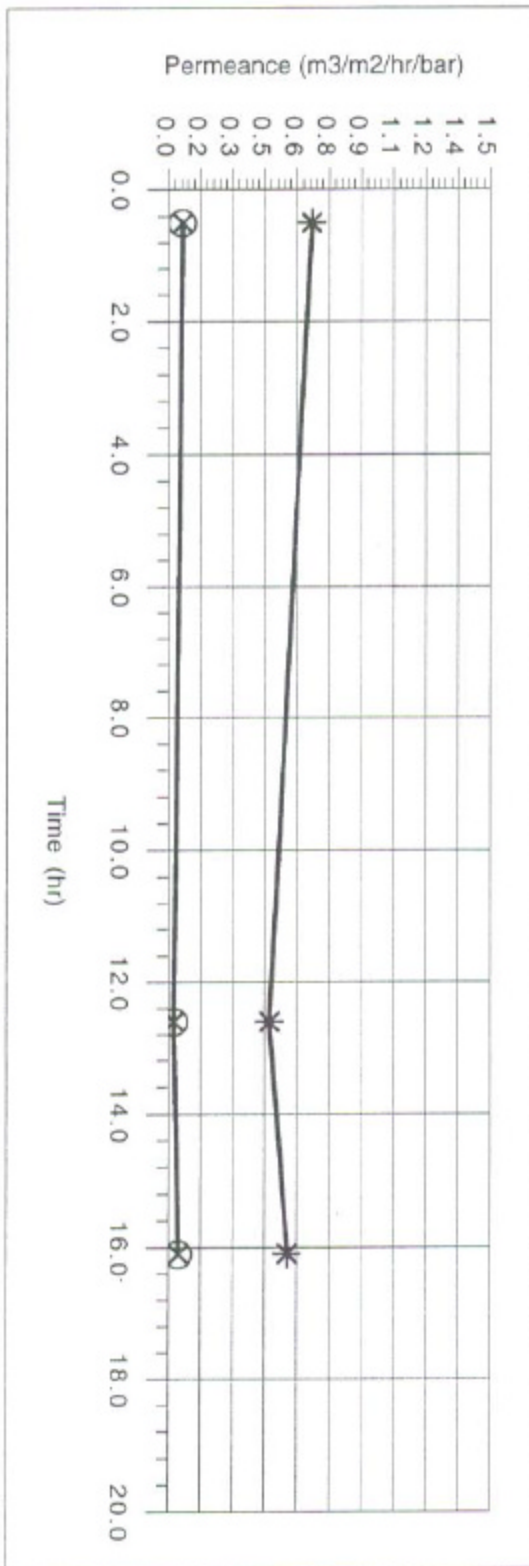
Figure 20. SEM photomicrograph of the SiC membrane after oxidation at 400°C in air for two hours. The SiC membrane after oxidation shows its original black color, indicative of the presence of SiC. The SEM photomicrograph here shows no visible difference before and after oxidation.

Figure 21. Permeance and Selectivity vs. Temperature for One of SiC Membranes (TPS-006B) Produced in Year I Study



Note: See Table 2 for performance of other SiC membranes produced from Phase I.

Figure 22. Permeance of SiC Membrane at 450°C and 30% Steam Membrane After Post-Treated to Remove Excess Carbon



⊗ N<sub>2</sub> (m<sup>3</sup>/m<sup>2</sup>/hr/bar) \* He (m<sup>3</sup>/m<sup>2</sup>/hr/bar)

He and N <sub>2</sub> Permeances before and after excess carbon removal from SiC membrane				
Temperature (°C)	He (m <sup>3</sup> /m <sup>2</sup> /hr/bar)	N <sub>2</sub> (m <sup>3</sup> /m <sup>2</sup> /hr/bar)	Selectivity	
Before	750	0.45	0.09	4.85
After	750	1.31	0.06	22.00

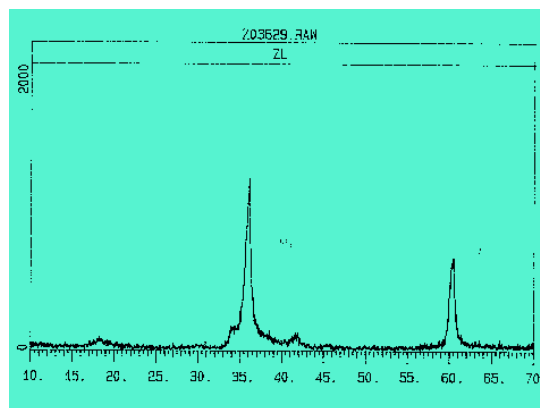


Figure 23a. XRD pattern of SiC powder (prepared from Sol6) before the hydrothermal stability test at 350° C and 50% steam (ambient pressure).

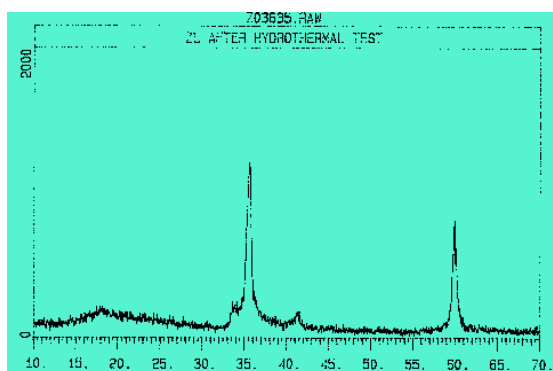


Figure 23b. XRD pattern of SiC powder (prepared from Sol6) after the hydrothermal stability test at 350° C and 50% steam (ambient pressure).

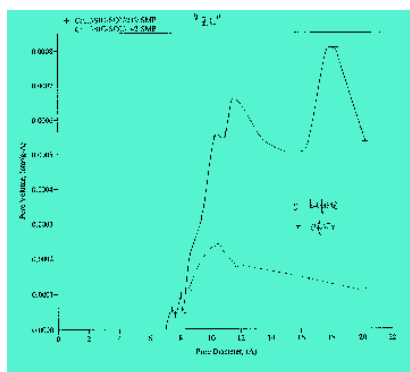


Figure 24. Pore size distribution of SiC powder (prepared from Sol6) before and after hydrothermal stability test at 350° C and 50% steam (ambient pressure).

Figure 25a. Hydrothermal Stability Test of Silicon Carbide Membrane (TPS-021) at 750°C and 50% Steam (atmospheric pressure)

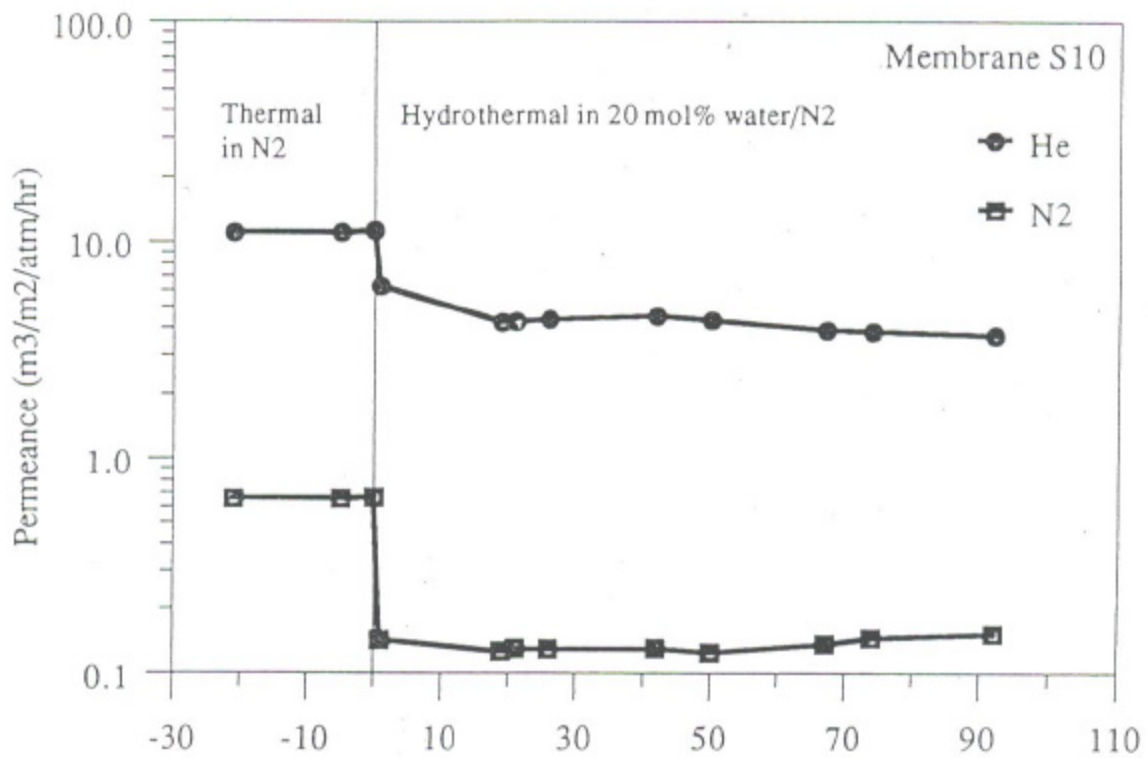
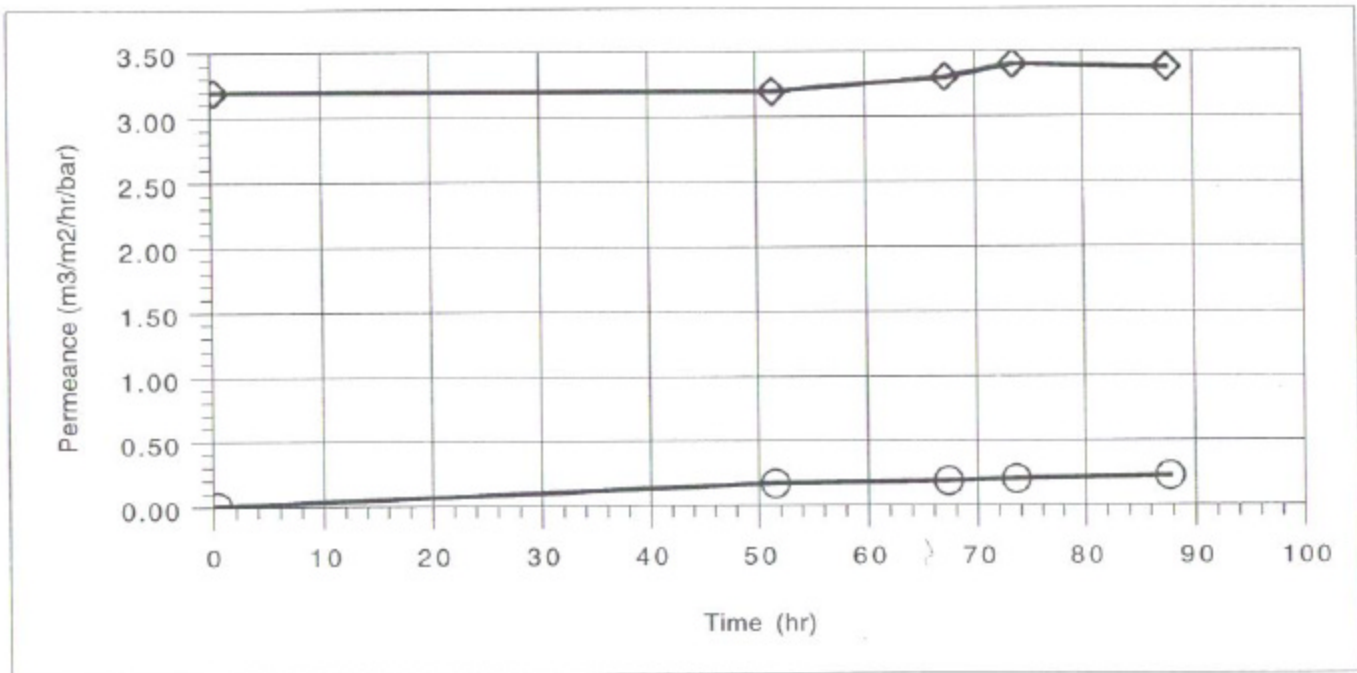
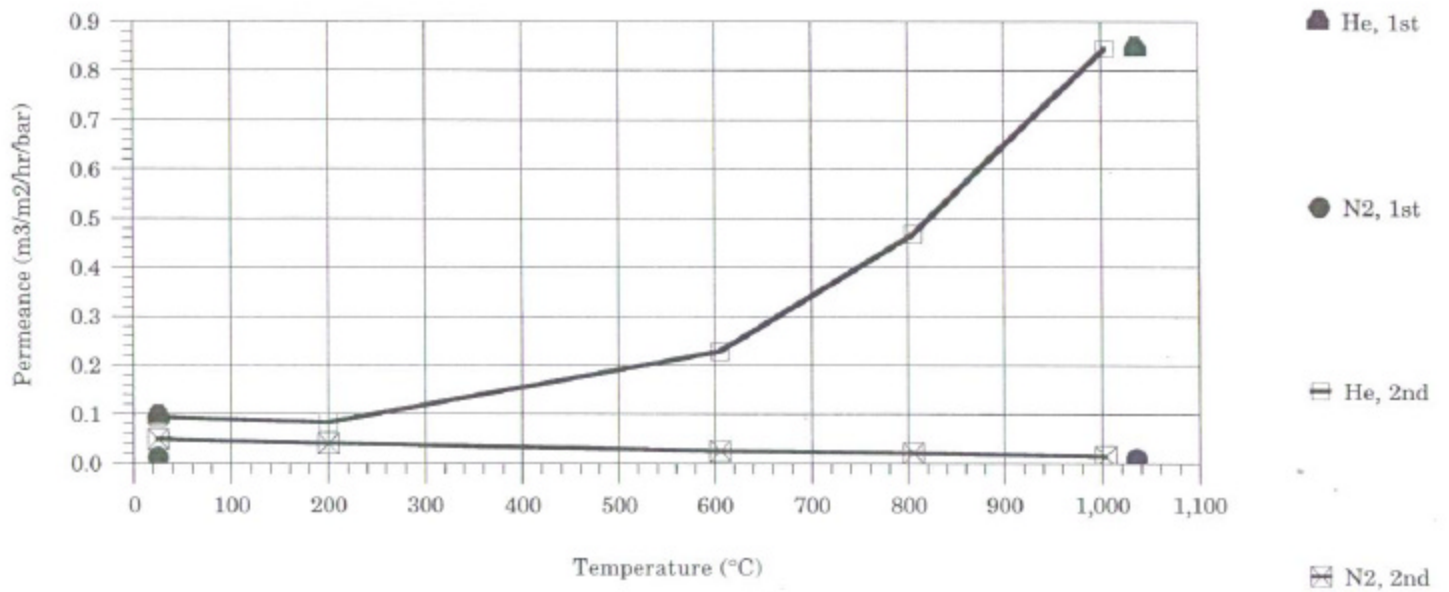
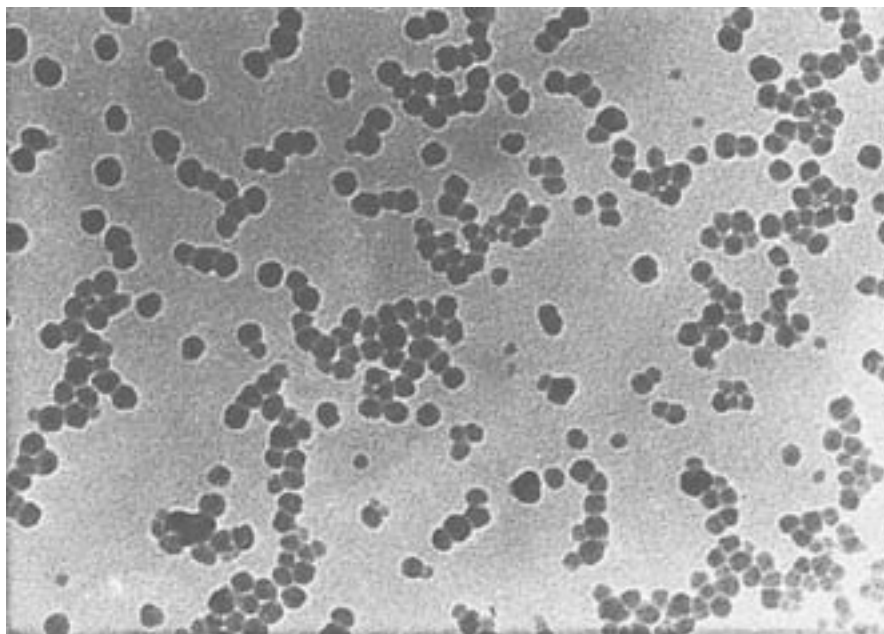


Figure 25b. Helium and nitrogen permeance of SiO<sub>2</sub> membrane stability test at 600°C and 20% steam (for comparison).

Figure 26. Effect of thermal cycling on SiC membrane (TPS-006B) supported on Al<sub>2</sub>O<sub>3</sub> Membrane: Assessment of Thermal Mismatch Between SiC and Al<sub>2</sub>O<sub>3</sub>



Note: The 1st cycle represents cooling from 1,000 (initial conversion to SiC after CVD deposition) to 25°C.  
 The 2nd cycle represents reheating from 25 to 1,000°C after the sample cooled to 25°C.



**Figure 27** The TEM picture of the organo-silica sol type IPAST with particle size 8-11 nm, provided by Nissan Chemical Industries, Ltd.

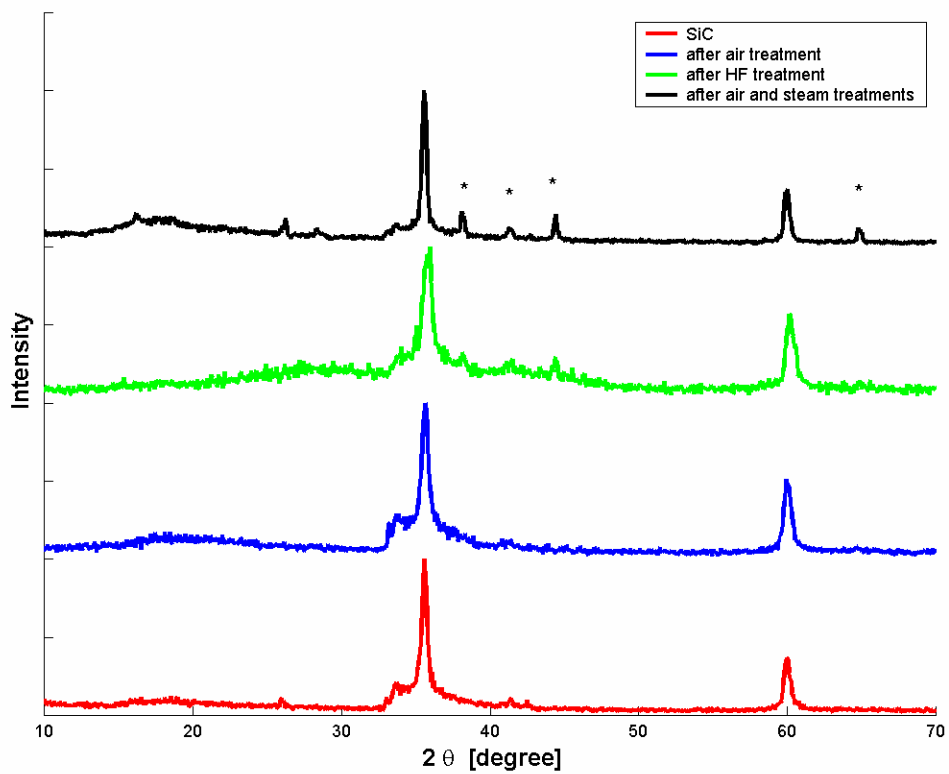


Figure 28. The XRD pattern of a SiC powder treated with HF, air, and steam. \* signifies the peaks corresponding to the (6H) phase.

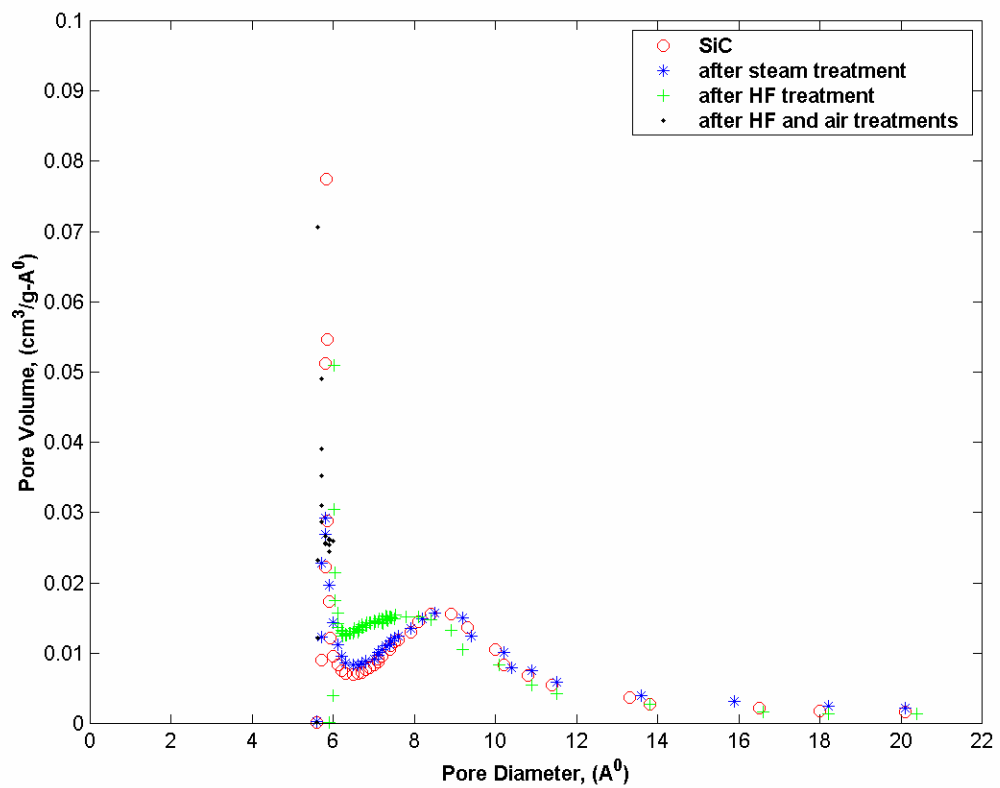
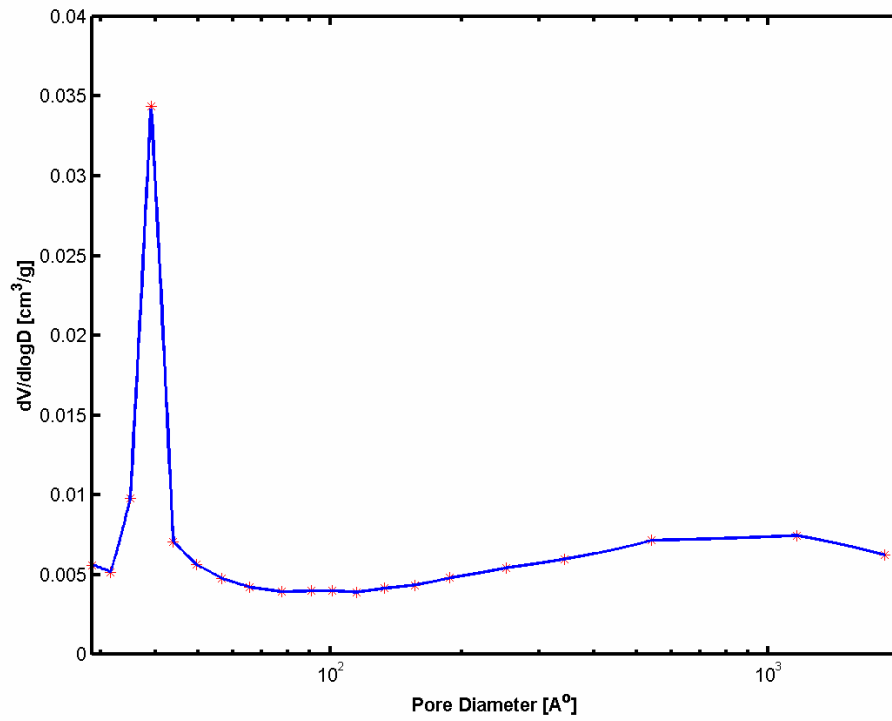
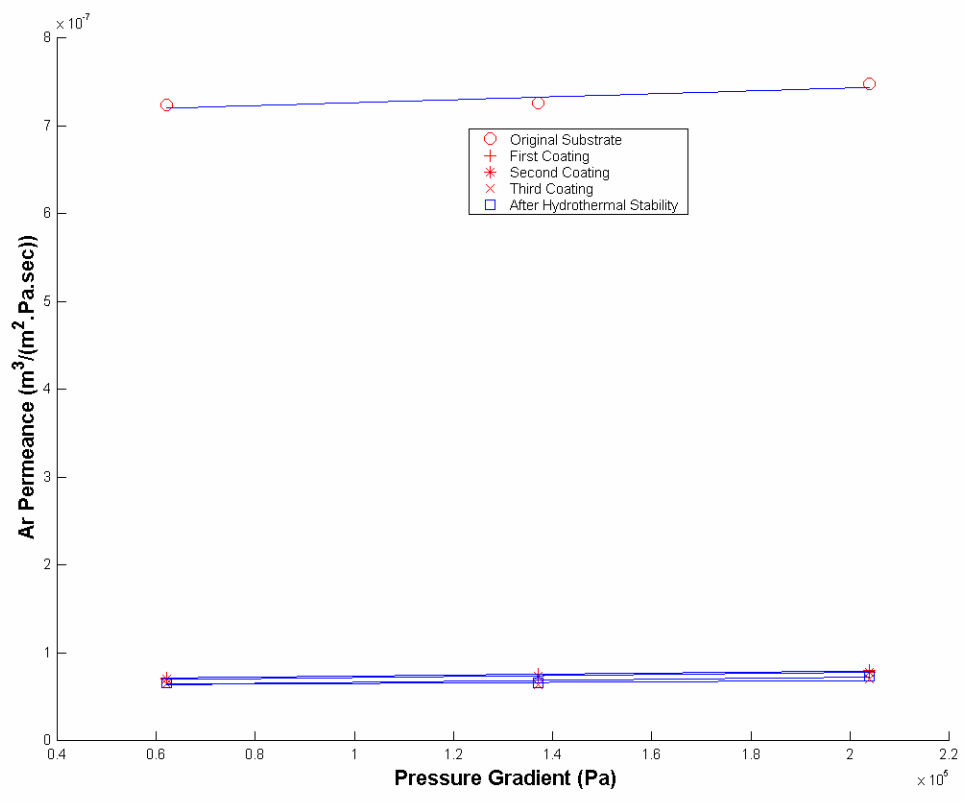


Figure 29. The pore size distribution of the SiC powders after various treatments



**Figure 30** The  $dV/d\log D$  of the SiC substrate utilized in the preparation of the Sol-Gel membranes.



**Figure 31.** The argon permeance of the membrane as a function of the pressure gradient and the number of coatings.

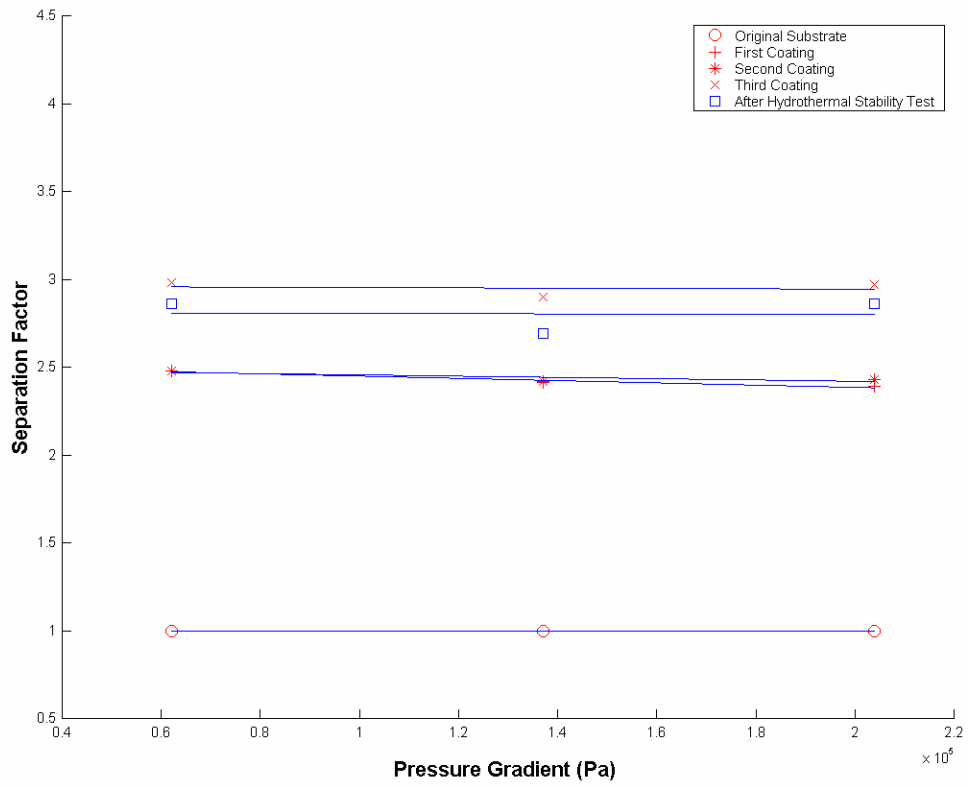


**Figure 32.** The separation factor of the membrane as a function of the pressure gradient and the number of coatings.

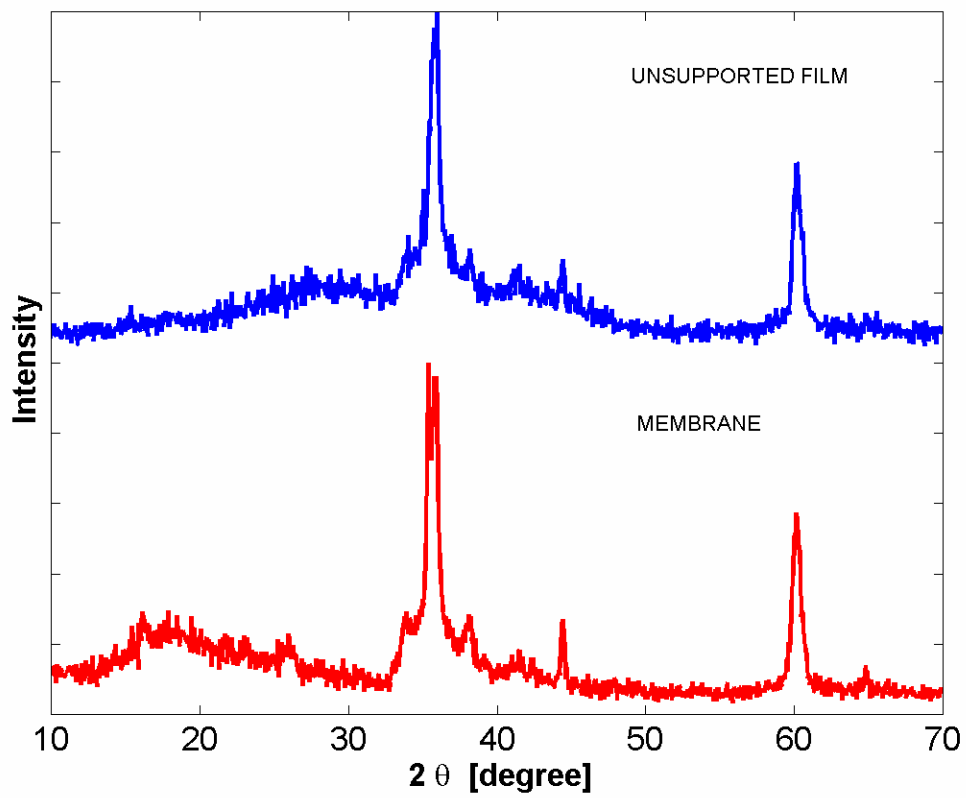


**Figure 33** The XRD patterns of the SiC membrane and the unsupported film (powder) prepared by the same techniques.

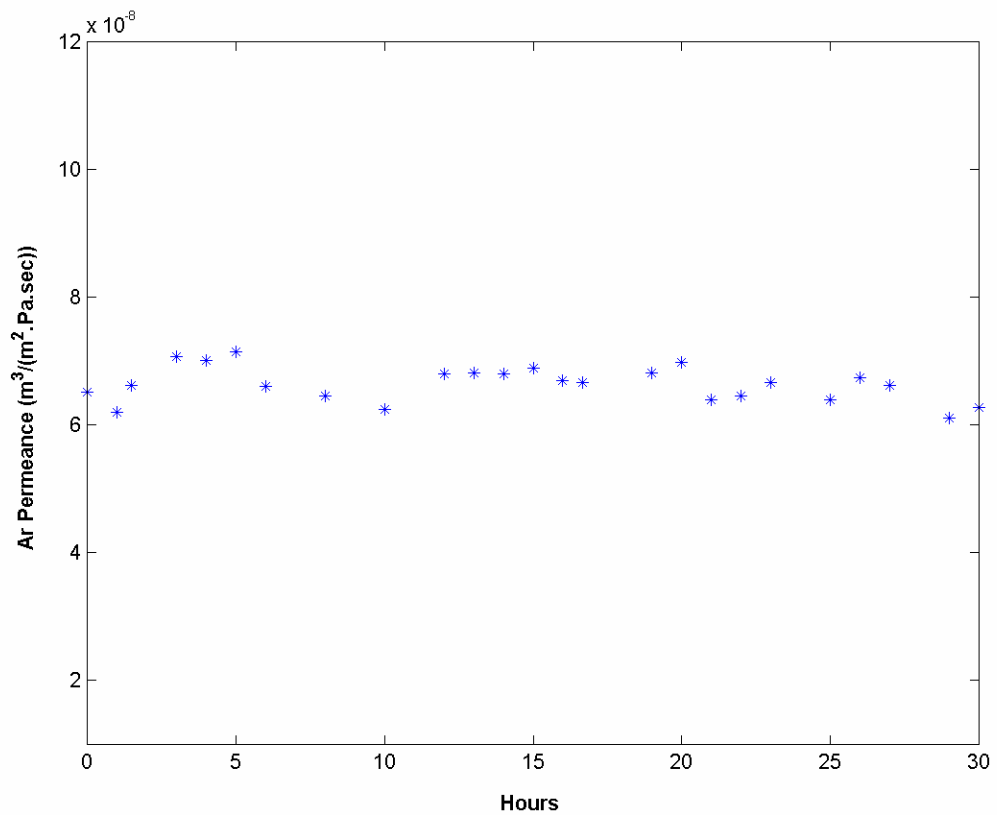


**Figure 34. The membrane argon permeance during exposure to steam.**

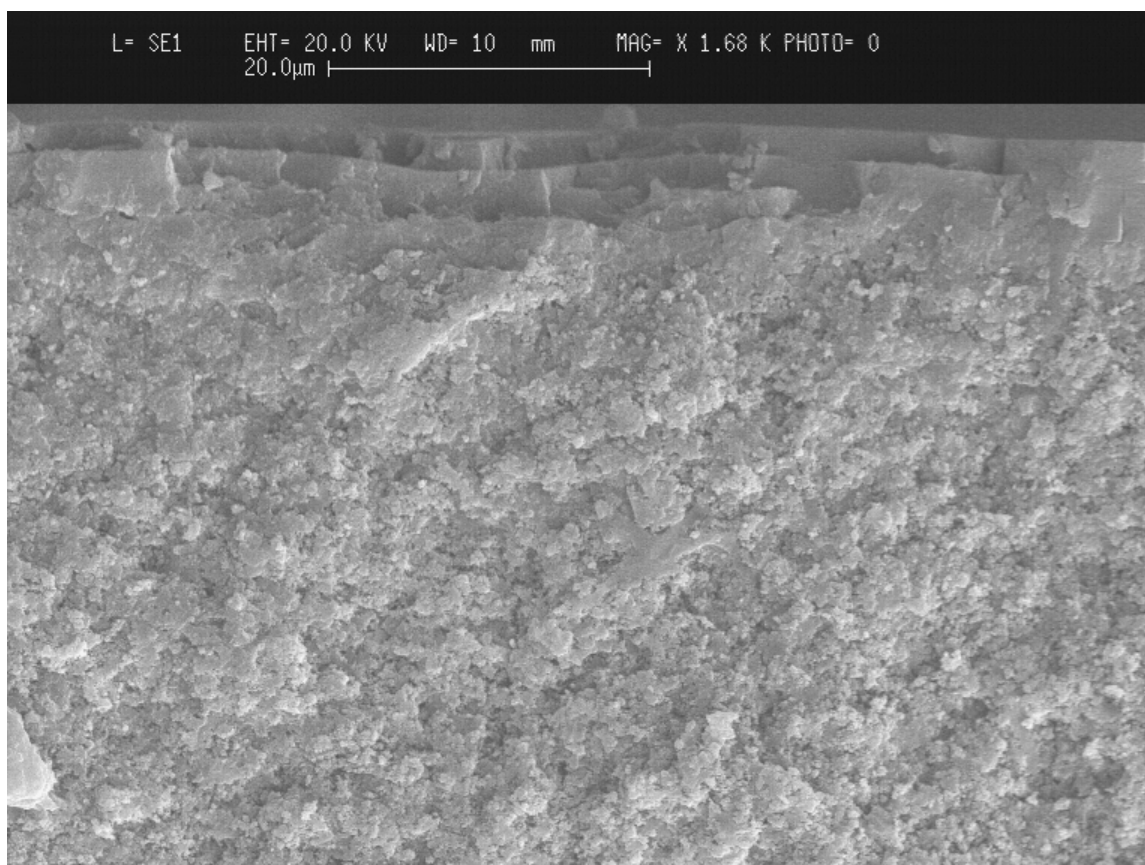


**Figure 35.** A SEM picture of the cross section of the SiC membrane prepared by Sol-Gel technique

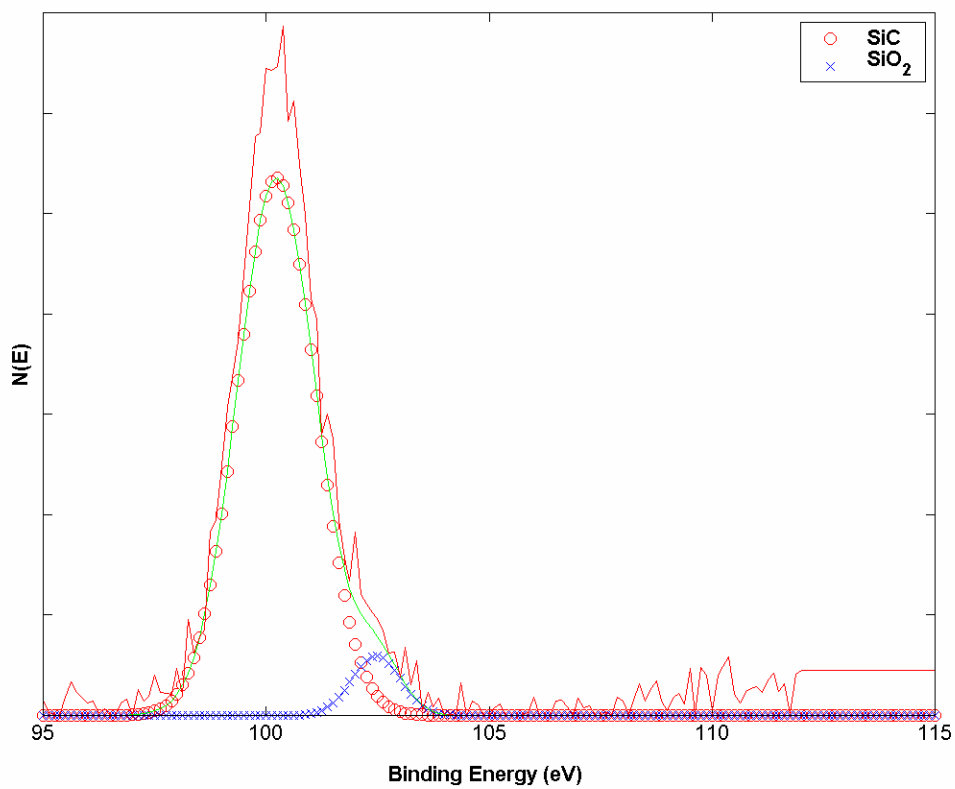


**Figure 36.** The XPS spectrum of the SiC powder sample. The superimposed peaks correspond to SiC at 100.4-101.0 eV and SiO<sub>2</sub> at 103.0-103.3 eV, respectively.

Figure 37 Performance of M&P Hydrogen Selective Membrane (U-130) and its Storage Stability (presented in terms of H<sub>2</sub> Permeance)

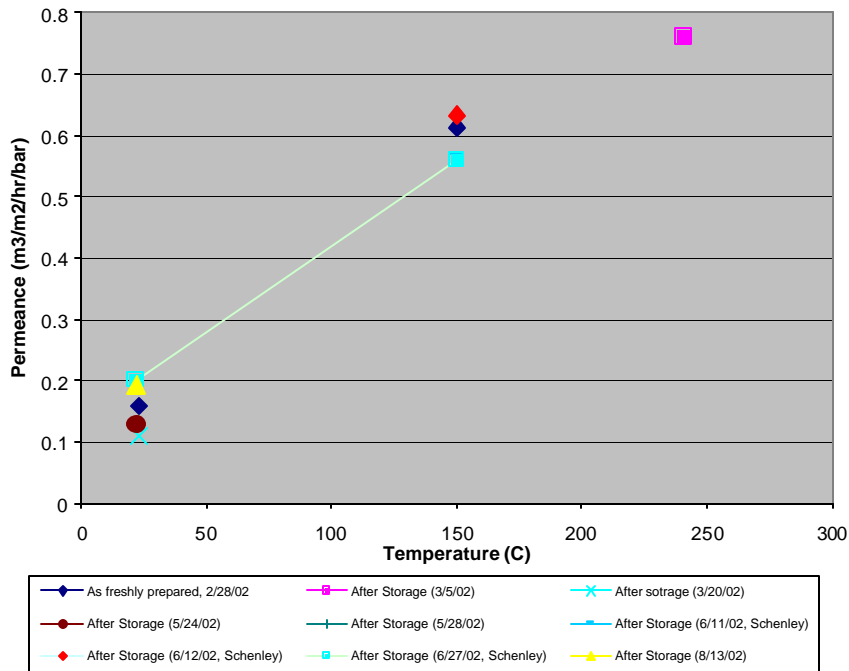
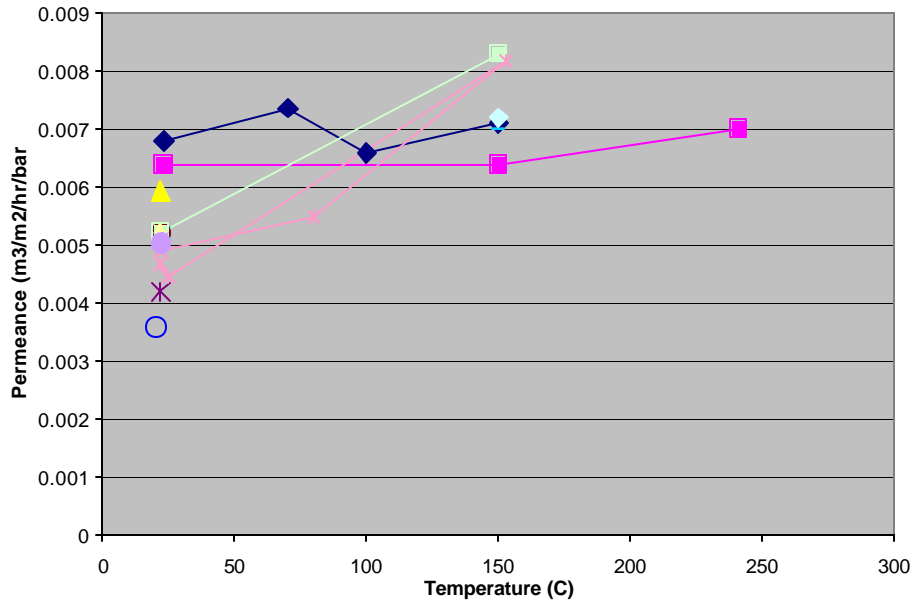
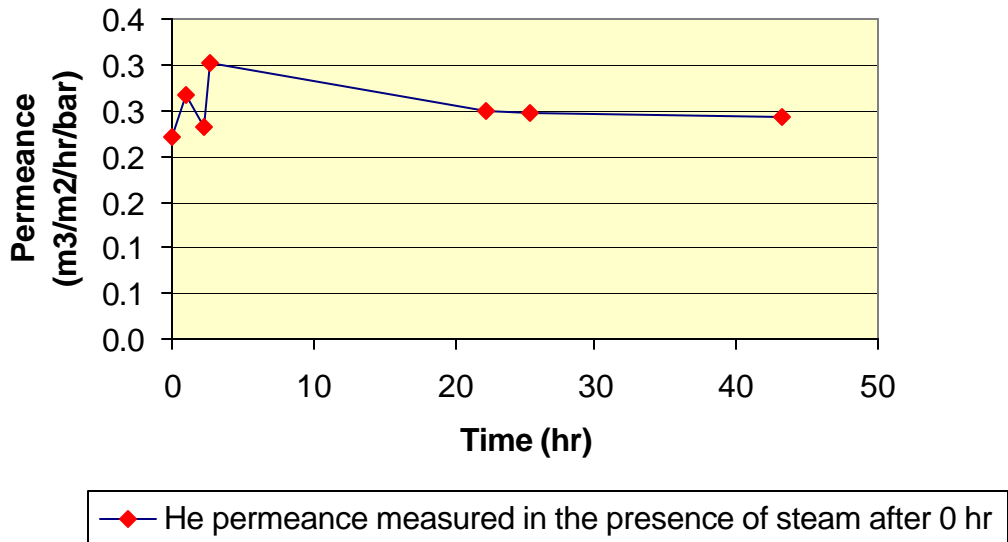


**Figure 38 Performance of M&P Hydrogen Selective Membrane and its Long Term Storage Stability (U-130): in terms of Nitrogen Permeance**



- ◆ As freshly prepared, 2/28/02
- ◆ After Storage (3/5/02)
- ▲ After Storage (3/6/02)
- ◆ After sotrage (3/20/02)
- ◆ After Storage (3/26/02)
- After Storage (5/24/02)
- ◆ After Storage (5/28/02)
- After Storage (6/7/02, UPARC)
- ◆ After Storage (6/11/02, Schenley)
- ◆ After Storage (6/12/02, Schenley)
- ◆ After Storage (6/27/02, Schenley)
- ◆ After Storage (6/28/02, Schenley)
- ◆ After Storage (7/3/02, UPARC)
- ◆ After Storage (7/16/02, UPARC)
- After Storage (8/13/02)

**Figure 39 Hydrothermal Stability Test of M&P Hydrogen Selective Membrane (200+/-5C with 3+/-0.5bar steam)**



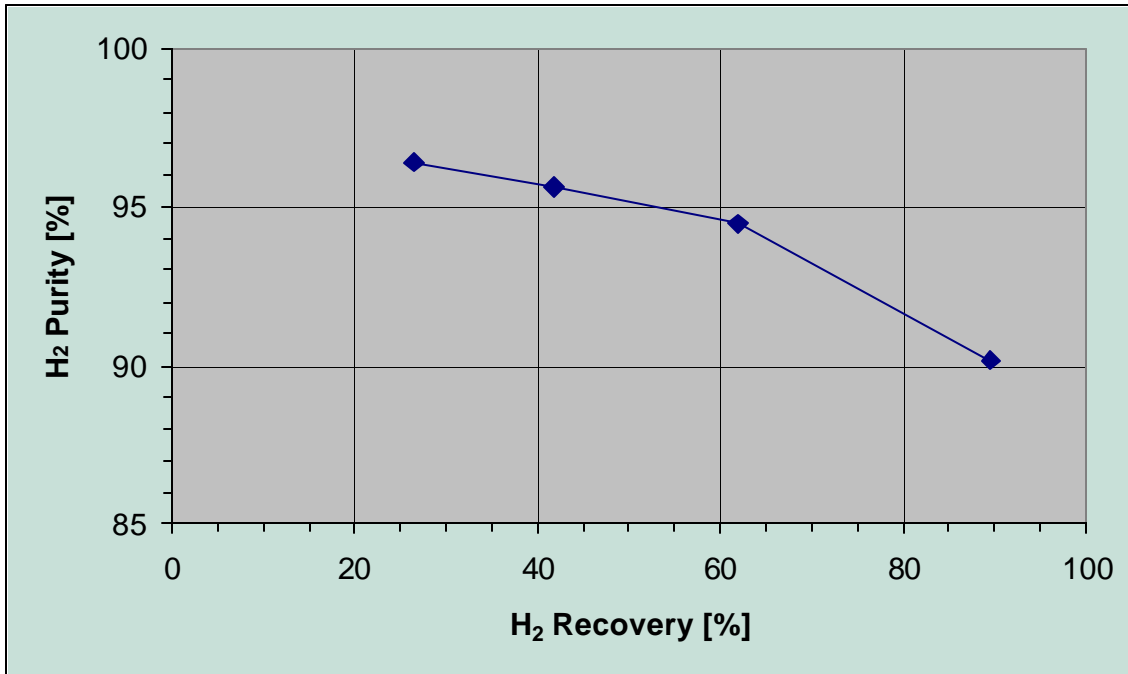
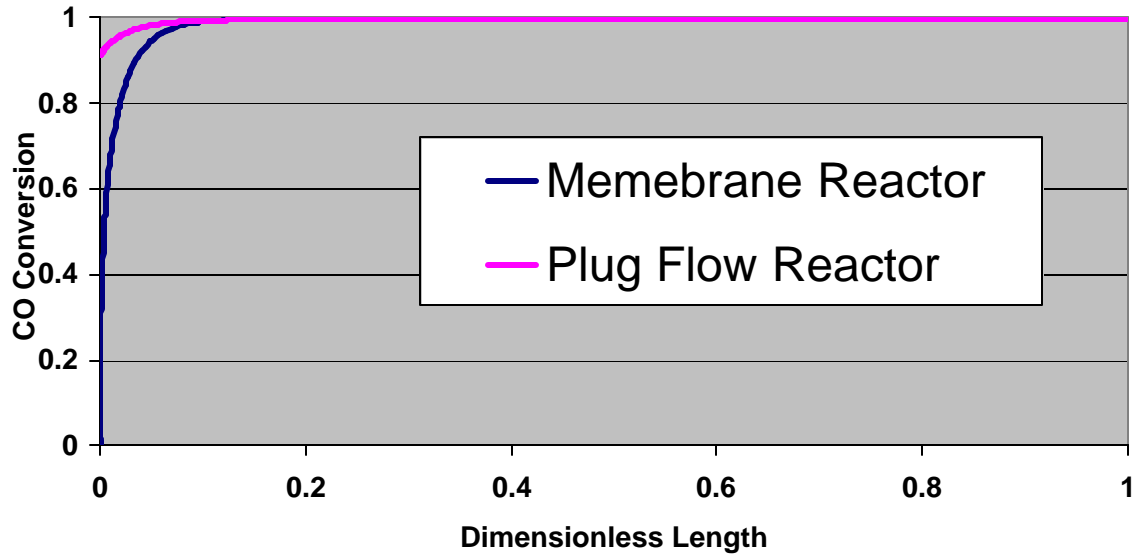


Figure 40 Hydrogen purity plotted as a function of hydrogen recovery for a full-scale M&P hydrogen selective membrane at 150°C and 100 psig. The feed is 50/50 H<sub>2</sub>/CO. The hydrogen permeance is 0.69 m<sup>3</sup>/m<sup>2</sup>/hr/bar and selectivity of H<sub>2</sub>/CO is 71 of the membrane used in this example.

**Figure 41 CO Conversion in Packed bed vs Membrane Reactor**  
250C, 13.6 atm (reactor side), 1 atm (permeate side),  
3 sec, Sweep Ratio=0.25



**Figure 42 CO Conversion through WGS: Effect of Steam/CO Ratio  
(same condition as above)**

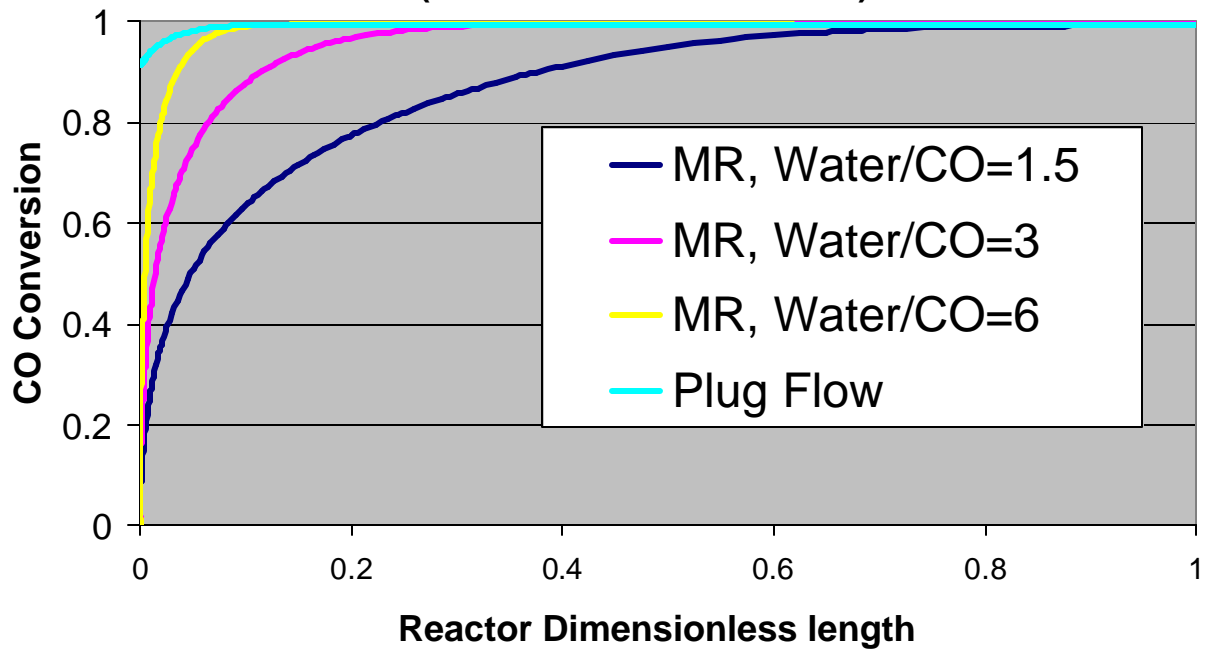


Figure 43 Effect of Steam/CO ratio for Hydrogen Recovery in Membrane reactor (same condition as above)

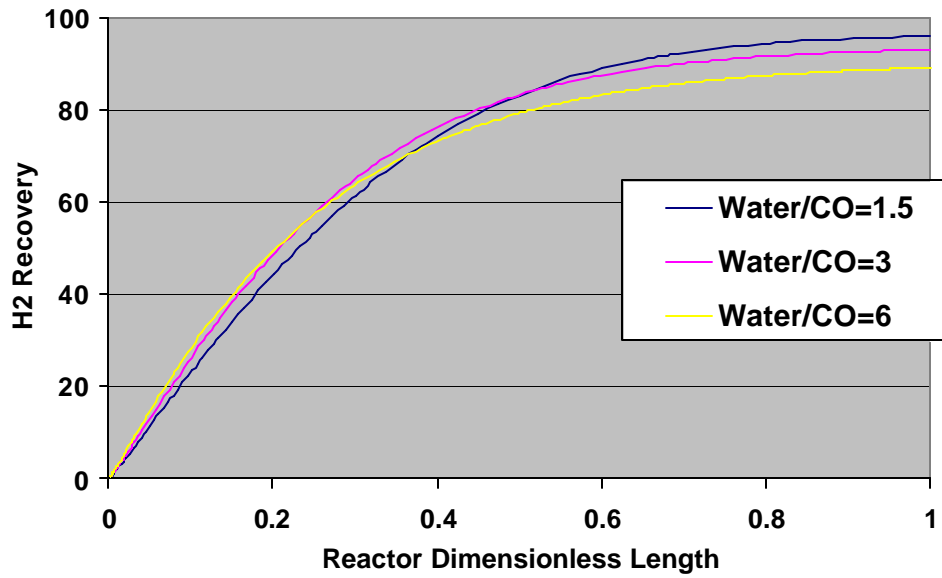
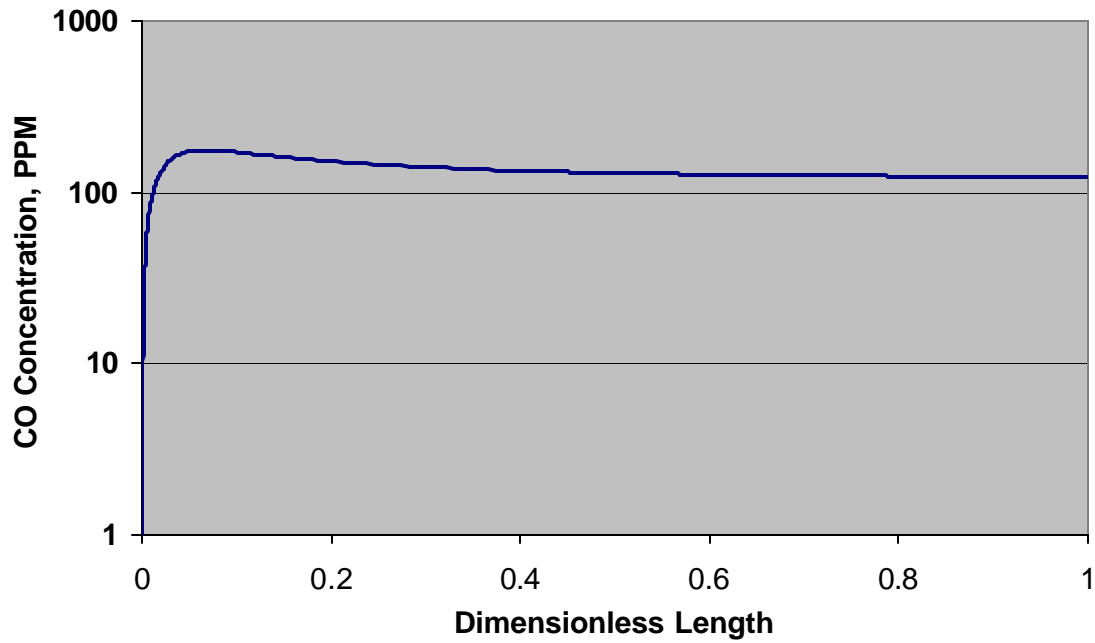


Figure 44 CO Concentration in H<sub>2</sub> Recovered from Membrane Reactor (same condition as above)



## **BIBLIOGRAPHY**

1. Puhlfurss, P.; Voigt, A.; Weber, R.; Morbe, M.; "Microporous TiO<sub>2</sub> Membranes with a cut off < 500 Da.," *Journal of Membrane Science*. 2000, 174[1], 123.
2. Wu, L.Q.; Huang, P.; Xu, N.P.; Shi, J.; "Effects of Sol Properties and Calcination on the Performance of Titanium Tubular Membranes, *Journal of Membrane Science*. 2000, 173[2], 263.
3. De Vos, R.M.; Maier, W.F.; Verweij, H.; "Hydrophobic silica membranes for gas separation, *Journal of Membrane Science*. 1999, 158[1-2], 277.
4. Kim, J.; Lin, Y.S.; "Sol-Gel synthesis and Characterization of Yttria-Stabilized Zirconia Membranes," *Journal of Membrane Science*. 1998, 139, 75.
5. Delange, R.S.A.; Hekkink, J.H.A.; Keizer, K.; Burggraaf, A.J.; "Microstructural Properties of Non-Supported Microporous," *Journal of Non-Crystalline Solids*. 1996, 195, 203.
6. Kim, K.S.; Jung, I.H.; "The permeability characteristics of non-porous membrane by C<sub>7</sub>H<sub>5</sub>F<sub>3</sub>/SiH<sub>4</sub> plasma polymeric membrane," *Korean Journal of Chemical Engineering*. 2000, 17[2] 149.
7. Drzal, P.L.; Halasa, A.F.; Kofinas, P.; "Microstructure orientation and nanoporous gas transport in semicrystalline block copolymer membranes," *Polymer*. 2000, 41[12] 4671.
8. Sea, B.K.; Ando, K.; Kusakabe, K.; Morooka, S.; "Separation of Hydrogen from Steam Using a SiC-Based Membrane Formed by Chemical Vapor Deposition of Tri-isopropylsilane," *Journal of Membrane Science*, 1998, 146, 73.
9. Takeda, Y; Shibata, N; Kubo, Y; "SiC coating on porous gamma-Al<sub>2</sub>O<sub>3</sub> using alternative-supply CVI method," *Journal of the Ceramic Society of Japan*, 2001, 109(4), 305.
10. Lee, L.; Tsai, D.S.; "Silicon Carbide Membranes Modified by Chemical Vapor Deposition Using Species of Low-Sticking Coefficients in a Silane/Acetylene Reaction System," *Journal of American Ceramic Society*. 1998, 81[1] 159.
11. Suwanmethanond, V.; Goo, E.; Johnston, G.; Liu, P.; Sahimi, M.; Tsotsis, T.T.; "Porous SiC Sintered Substrates for High Temperature Membranes for Gas Separations," *Journal of Industrial & Engineering Chemistry Research*. 2000, 39[9], 3264.
12. Cerovic, L.J.; Milonjic, S.K.; Zec, S.P.; "A Comparison of Sol-Gel Derived Silicon Carbide Powders from Saccharose and Activated Carbon," *Ceramics International*. 1995, 21, 271.
13. Seog I.S.; Kim, C.H.; "Preparation of Monodispersed Spherical Silicon Carbide by the Sol-Gel Method," *Journal of Materials Science*. 1993, 28, 3277.
14. Raman, V.; Bahl, O.P.; Dhawan, U.; "Synthesis of Silicon Carbide through the Sol-Gel Process from Different Precursors" *Journal of Material Science*. 1995, 30, 2686.
15. Schubert, U.; Husing, N.; in *Synthesis of Inorganic Materials*, WILEY-VCH, Weinheim 2000, ch.2.
16. Weimer, A.W.; Nilsen, K.J.; G.A. Cochran, G.A.; Roach, R.P.; "Kinetics of Carbothermal Reduction of Beta Silicon Carbide", *AIChE Journal*. 1993, 39, 493.
17. Meng, G.W.; Zhang, L.D.; Mo, C.M.; Zhang, S.Y.; Qin, Y.; Feng, S.P.; Li, H.J.; "Synthesis of "A β-SiC Nanorod with SiO<sub>2</sub> Nanorod" One Dimensional Composite Nanostructures", *Solid State Communications*. 1998, 106[4], 215.
18. Bootsma, G.A.; Knippenberg, W.F.; and Verspui, G.; *Journal of Crystal Growth*. 1971, 8, 341.
19. Kraft, T.; Nickel, K.G.; "Hydrothermal Degradation of Chemical Vapour Deposited SiC Fibres", *Journal of Materials Science*, 1998, 33[17], 4357
20. Alvin, M.A., "High Temperature Gas Cleaning", Vol. II, 1999, edit by A. Dittler, G. Hemmer, and G. Kasper, Universitat Karlsruhe.Bracht, M., Alderliesten, P.T., Kloster,
21. R. Pruschker, R., Haupt, G., Xue, E., Ross, J.R., Koukou, M.K., Papayannakos, N., Energy Conservation and Management, 38, S159 (1997).
22. L.J. Cerovic, S.K. Milonjic and S.P. Zec, "A Comparison of Sol-Gel Derived Silicon Carbide Powders from Saccharose and Activated Carbon," Ceramics International, 21 271-276 (1995).
23. Lee, L., and Tasi, D., J. Am. Ceram. Sci., 81, 159 (1998).
24. Liu, P.K.T., and Wu, J.C.S., US Patent 5,415,891, May 16, 1995.
25. Megiris, C., and Glezer, J. H., Ind. Eng. Chem. Res., 31, 1293(1992)
26. V. Raman, O.P. Bahl, and U. Dhawan, "Synthesis of Silicon Carbide through the Sol-Gel Process from Different Precursors" *Journal of Material Science*, 30 2686-2693 (1995).
27. Sea, B.K., Ando, K., Kusakabe, K., and Morooka, S., J. Membrane Science, 146, 73 (1998).
28. I.S. Seog and C.H. Kim, "Preparation of Monodispersed Spherical Silicon Carbide by the Sol-Gel Method," Journal of Materials Science, 28 3277-3282 (1993).

29. Stiegel, G., "A New IGCC Program Strategy to Meet Future Energy Market Requirements", Advanced Coal-Based Power and Environmental Systems '98 Conference, FETC.
30. V. Suwanmethanond, E. Goo, G. Johnston, P. Liu, M. Sahimi, and T.T. Tsotsis, "Porous SiC Sintered Substrates for High Temperature Membranes for Gas Separations," Ind. Eng. Chem. Res., **39**, 3264-3271 (2000).
31. Wu, J.C.S., Sabol, H., Smith, G.W., Flowers, D.F., Liu, P.K.T., J. Membrane Sci., **96**, 275 (1994).
32. Satterfield, C. N., Heterogeneous Catalysis in Practice, McGraw-Hill, 1980.

## LIST OF ACRONYMS AND ABBREVIATIONS

AFM:	Atomic Force Microscopy
AHPCS:	Allyl-hydridopoly Carbosilane
CVD/I:	Chemical Vapor Deposition/Infiltration
HF:	Hydrofluoric Acid
HTS:	high temperature shift
LTS:	low temperature shift
MR:	Membrane Reactor
PAN:	Polyacrylonitrile
PCS:	Polycarbon Silane
PSD:	Pore size distribution
PTMS:	Phenyltrimethoxysilane
SEM:	Scanning Electron Microscopy
TEOS:	Tetraethylorthosilicate
TPS:	Tripropyl Silane
WGS:	Water-Gas-Shift
XPS:	X-Ray Photospectroscopy
XRD:	X-Ray Diffraction

## APPENDICES

1. Publication as a result of current research under this project:

V. Suwanmethanond, E. Goo, G. Johnston, P. Liu, M. Sahimi, and T.T. Tsotsis, "Porous SiC Sintered Substrates for High Temperature Membranes for Gas Separations," Ind. Eng. Chem. Res., 39, 3264-3271 (2000).

R. Ciora, B. Fayyaz, P. Liu, V. Suwanmethanond, R. Mallada, M. Sahimi, and T.T. Tsotsis, "Preparation and Reactive Applications of Nanoporous Silicon Carbide Membranes," ISCRE 18.